

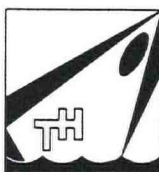


**THE DISTRIBUTION OF HYDRODYNAMIC MASS
AND DAMPING OF AN OSCILLATING SHIPFORM
IN SHALLOW WATER**

W. Beukelman and Prof.ir. J. Gerritsma

**Conference on Behaviour of Ships in Re-
stricted Water, Eleventh Scientific and
Methodological Seminar on Ship Hydrody-
namics, Bulgarian Ship Hydromechanics
Centre, Varna, 11 - 13 November 1982.**

Report No. 546-P March 1982
Ship Hydromechanics Laboratory - Delft



Delft University of Technology
Ship Hydromechanics Laboratory
Mekelweg 2
2628 CD DELFT
The Netherlands
Phone 015 -786882

"This report is prepared by THD/WL/NSP under contract no. 82/1528/7.3. of the Stichting Coördinatie Maritiem Onderzoek."

"© THD/WL/NSP, 1982."

"Reproduction in whole or in part by means of print, photocopy, microfilm or in any other way is only permitted after
preceding written consent of THD/WL/NSP."



БОЛГАРСКИЙ ИНСТИТУТ ГИДРОДИНАМИКИ СУДНА

BULGARIAN SHIP HYDRODYNAMICS CENTRE

КОНФЕРЕНЦИЯ - ПОВЕДЕНИЕ СУДОВ В ОГРАНИЧЕННОМ ФАРВАТЕРЕ -

CONFERENCE ON BEHAVIOUR OF SHIPS IN RESTRICTED WATERS

ДОКЛАДЫ, Том I

PROCEEDINGS, Volume I

Одиннадцатый научно - методологический семинар гидродинамики судна
Eleventh Scientific and Methodological Seminar on Ship Hydrodynamics

Варна 11 ÷ 13.11.1982 Varna



THE DISTRIBUTION OF HYDRODYNAMIC MASS
AND DAMPING OF AN OSCILLATING SHIPFORM
IN SHALLOW WATER

W. Beukelman, J. Gerritsma

Introduction

The depth of water has an important influence on the vertical and horizontal motions of a ship in waves, in particular when the waterdepth is smaller than two and a half times the draught of the vessel.

In shallow water the keel clearance depends to a large extent on the combined effects of trim, sinkage and the vertical displacement of the ship's hull as a result of the ship motions in waves. Keel clearance is of interest to ship owners and port authorities, because of the increasing draught of large cargo ships and the corresponding smaller waterdepth/draught ratio's. The safety and manoeuvrability of a ship are influenced by the amount of keel clearance and the cost of dredging depends to a large extent on the allowable minimum keel clearance of the largest ships considered.

A detailed knowledge of the vertical motions of a ship due to waves in shallow water will be of interest to assist in solving such problems.

From a technical point of view strip theory methods to calculate ship motions due to waves in deep water have proved to give satisfactory results. Except for the rolling motions, viscous effects are not important in strip theory calculations, but an accurate determination of 2-dimensional damping and added mass of ship-like cross sections is necessary, as shown earlier [1].

In the case of shallow water the use of strip theory calculations is not obvious, because a much larger influence of viscosity can be expected when the keel clearance is small. In addition, the flow conditions near the bow and the stern will differ to a large extent from the two-dimensional flow assumption, as used in the strip theory.

The present investigation concerns the comparison of the distribution of hydrodynamic mass

and damping, as measured on a segmented ship model in shallow water, with corresponding calculated results using a strip theory method which takes the finite waterdepth into account.

It should be noted that in these calculations no viscosity effects have been included.

In view of the comparison with calculations the physical model has been restrained from sinkage and trim, which would occur in the case of a free floating model. In addition to the heaving and pitching motions also forced horizontal motions in the sway and yaw mode have been carried out.

The experiments included the effects of forward speed, frequency of oscillation and waterdepth. A range of frequencies have been chosen to cover wave frequencies of interest for ship responses.

The use of a segmented ship model enables the determination of the sectional values of damping and added mass. This technique has been used earlier for an analogous investigation of the deep water case [1].

See appendix 1.

The calculations have been carried out with a computer program developed by H. Keil [3].

In this calculation the hydrodynamic mass and damping for 2-dimensional ship-like cross sections are computed with potential flow theory, using a source and a linear combination of multipole potentials, which satisfy the boundary conditions at the free surface, the bottom, and the contour of the cross section. A Lewis transformation has been used to generate ship-like cross sections.

The model.

The forced oscillation experiments have been carried out with a 2.3 meter model of the Sixty Series. The main particulars are given in Table 1. The same model has been used earlier for the analogous tests in deep water [1,2]. The model has been divided in seven segments each of which was separately connected to strong beam by means of a strain gauge dynamometer.

Table 1.

Length between perpendiculars	L_{pp}	2.258 m
Length on the waterline	L_{WL}	2.296 m
Beam	B	0.322 m
Draught	T	0.129 m
Volume of displacement	∇	0.0657 m ³
Block coefficient	C_B	0.700
Waterplane area	A_{WL}	0.572 m ²
Longitudinal moment of inertia of waterplane	I_{WL}	0.1685 m ²
LCB forward of $L_{pp}/2$		0.011 m
LCF aft of $L_{pp}/2$		0.038 m

Table 2a. Heave

$\omega = 4,6,8,10,12$ rad/s					r (m)
h/T					
2.40	1.80	1.50	1.20	1.15	
.	0.005
.	0.010
.	0.020
.	0.030

. Fn = 0.1 and 0.2

Table 2b. Pitch

$\omega = 4,6,8,10,12$ rad/s					r (m)
h/T					
2.40	1.80	1.50	1.20	1.15	
.	0.005
.	0.010
.	0.015

. Fn = 0.1 and 0.2

x Fn = 0.2 only

Table 2c. Sway and yaw

$\omega = 4,6,8,9,10$ rad/s					r (m)
h/T					
2.4	1.8	1.5	1.2	1.15	
.	0.010
.	0.020
.	0.030

. Fn = 0.1 and 0.2

These dynamometers measured vertical or horizontal forces only.

The test set up for vertical motions is given in Figure 1. A similar system has been used for the horizontal motions, see Figure 2.

The instrumentation allowed the determination of in-phase and quadrature components of the vertical or horizontal forces on each of the seven segments when they perform forced harmonic motions with a given amplitude and frequency.

It has been shown earlier that the influence of the gaps between segments can be neglected. [2].

Test conditions.

The various oscillation amplitudes cover a certain range, depending on the mode of motion, to study the occurrence of non-linearities.

The test conditions are summarized in Table 2.

These conditions include the waterdepth-draught ratio h/T, the oscillator amplitude r, the frequency of oscillation ω and the forward speed, expressed as the Froude number Fn.

It should be noted that the distance between the two oscillator rods (see Figure 1) is one meter. Consequently for the pitch and the yaw modes a 0.01 meter oscillation amplitude corresponds to a 1.146 degree motion amplitude. The dimensionless frequency covers a range of

$$\omega \sqrt{L/g} = 1.9 - 5.8 \text{ for pitch and heave, and}$$

$$\omega \sqrt{L/g} = 1.9 - 4.8 \text{ for sway and yaw.}$$

Experimental results

For each of the considered modes of motion the in-phase and quadrature components of the exciting forces has been determined. These components have been elaborated to the hydrodynamic mass and hydrodynamic damping coefficient of each segment, taking into account the amplitude and frequency of the harmonic motion.

The following expressions have been used in this respect (see Appendix 1).

Heave:

$$(\rho \nabla + a_{zz}) \ddot{z} + b_{zz} \dot{z} + c_{zz} z - d_{z\theta} \ddot{\theta} - e_{z\theta} \dot{\theta} - g_{z\theta} \theta =$$

$$= F_z \sin(\omega t + \epsilon_z)$$

Pitch:

$$(I_{yy} + a_{\theta\theta}) \ddot{\theta} + b_{\theta\theta} \dot{\theta} + c_{\theta\theta} \theta - d_{\theta z} \ddot{z} - e_{\theta z} \dot{z} - g_{\theta z} z =$$

$$= M_\theta \sin(\omega t + \epsilon_\theta)$$

Sway:

$$(\rho v + a_{YY})\ddot{Y} + b_{YY}\dot{Y} - d_{Y\psi}\ddot{\psi} - e_{Y\psi}\dot{\psi} = F_Y \sin(\omega t + \epsilon_Y)$$

Yaw:

$$(I_{ZZ} + a_{\psi\psi})\ddot{\psi} + b_{\psi\psi}\dot{\psi} - d_{\psi Y}\ddot{Y} - e_{\psi Y}\dot{Y} = M_{\psi} \sin(\omega t + \epsilon_{\psi}) \quad (1)$$

For the individual segments the following equations result:

Heave:

$$(\rho v^* + a_{zz}^*)\ddot{z} + b_{zz}^*\dot{z} + c_{zz}^*z = F_z^* \sin(\omega t + \epsilon_z^*)$$

Pitch:

$$(\rho v^* x_i + d_{z\theta}^*)\ddot{\theta} + e_{z\theta}^*\dot{\theta} + g_{z\theta}^*\theta = -F_{\theta}^* \sin(\omega t + \epsilon_{\theta}^*)$$

Sway:

$$(\rho v^* + a_{YY}^*)\ddot{Y} + b_{YY}^*\dot{Y} = F_Y^* \sin(\omega t + \epsilon_Y^*)$$

Yaw:

$$(\rho v^* x_i + d_{Y\psi}^*)\ddot{\psi} + e_{Y\psi}^*\dot{\psi} = -F_{\psi}^* \sin(\omega t + \epsilon_{\psi}^*) \quad (2)$$

In these equations a refers to hydrodynamic mass, b is the hydrodynamic damping coefficient and c is a restoring force- or moment coefficient.

The coefficients d, e and g are the corresponding cross coupling coefficients. The position of a segment is denoted by x_i and values of the coefficients of segments are indicated by the asterisk *.

In Appendix 1 the data reduction of the results obtained from the oscillator experiments is treated in some detail.

The coefficients a, b, d and e have been obtained by integration over the length of the model of the results of the segments.

In the Fig. 3 to 26 the experimental values of hydrodynamic mass, damping and cross coupling coefficients are given for pitch, heave, yaw and sway as a function of the frequency of oscillation ω and the relative waterdepth h/T .

Two forwards speeds corresponding to $Fn = 0.1$ and $Fn = 0.2$ have been considered.

In general the experiments indicate a rather good linearity with regard to the amplitudes of motion, except some minor non-linearities at the smallest waterdepth.

Mass and damping coefficients of heave and pitch increase with decreasing waterdepth for all considered frequencies, in particular for $h/T < 1.5$.

For the lateral motions, sway and yaw, the hydrodynamic mass coefficients decrease with decreasing waterdepth, whereas the damping coefficients decrease slightly or are almost independent of waterdepth.

The distribution of the hydrodynamic mass and damping along the length of the model is given in the Figures 3 to 18 for heave, pitch, sway and yaw, as a function of frequency, waterdepth and forward speed. The distribution of the hydrodynamic mass, expressed as a percentage of the total hydrodynamic mass, is not greatly influenced by the waterdepth, but for the distribution of the damping coefficients a significant shift of larger damping values towards the fore body of the shipmodel with decreasing waterdepth is observed.

For low frequencies of oscillation, combined with low forwards speeds wall effects or oscillation in the models own wave-system could have influenced the measurements. This could explain some of the irregularities in case of the lowest speed $Fn = 0.1$ and frequencies equal or below $\omega = 6$ rad/s. In all other cases wall effects do not seem to have influenced the experimental results.

Calculated hydrodynamic mass and damping

The measured mass and damping values have been compared with the corresponding calculated values, according to the numerical procedure as given by Keil [3]. This concerns the coefficients a, b, d and e for the four considered modes of motion, as well as the distribution of these quantities along the length of the model.

The results are shown in the Figures 3 to 26.

In the strip theory the added mass and damping values at zero speed of advance are used to compose the coefficients of the equations of motion. The expressions for the sectional coefficients for heave and pitch as derived in [4] are given in Appendix 2 together with an analogous extension for sway and yaw.

Two versions of the strip theory have been used.

Version 1 leads to the ordinary strip theory method, which lacks some of the symmetry relations in the damping cross coupling coefficients.

Version 2 includes these additional terms. In general the calculated results according to both versions agree rather well except for the sectional values of the coefficients near the ends of the ship form.

For the integrated values of mass and damping the differences between version 1 and 2 may be neglected.

For zero forward speed the calculated values of added mass and damping are presented in table 3 for heave and sway, the different frequencies and the waterdepth- draught ratio's considered.

Table 3.

Calculated added mass and damping for heave and sway at zero speed

HEAVE Fn = 0

ω 1/s	h/T = 2.40		h/T = 1.80		h/T = 1.50		h/T = 1.20		h/T = 1.15	
	a_{zz}	b_{zz}	a_{zz}	b_{zz}	a_{zz}	b_{zz}	a_{zz}	b_{zz}	a_{zz}	b_{zz}
4	46.6	399.1	58.6	464.8	78.5	514.3	149.4	583.7	183.1	598.0
6	50.2	317.7	62.4	378.7	82.2	427.7	152.8	498.7	186.5	513.5
8	57.5	208.4	69.4	261.9	88.7	309.3	158.6	381.4	192.1	396.5
9	62.4	155.1	74.2	200.5	93.3	244.3	162.6	314.4	196.0	329.2
10	67.6	111.0	79.6	145.2	98.5	182.3	167.2	246.4	200.5	260.4
12	76.3	55.0	89.8	69.2	109.1	88.1	177.8	127.6	210.9	136.8

SWAY Fn = 0

ω 1/s	h/T = 2.40		h/T = 1.80		h/T = 1.50		h/T = 1.20		h/T = 1.15	
	a_{yy}	b_{yy}	a_{yy}	b_{yy}	a_{yy}	b_{yy}	a_{yy}	b_{yy}	a_{yy}	b_{yy}
4	78.7	188.4	73.1	259.3	66.3	323.0	50.0	428.5	45.0	453.5
6	53.2	364.9	43.6	386.9	36.2	412.9	24.9	463.0	22.3	475.5
8	24.8	450.5	21.8	435.6	18.5	434.1	13.5	450.8	12.3	455.4
9	15.6	433.4	14.6	422.8	13.1	419.4	10.4	430.7	9.7	432.1
10	10.5	396.2	10.2	392.4	9.6	391.5	8.5	402.8	8.1	400.1
12	7.7	313.2	7.6	314.2	7.5	317.2	7.7	331.8	7.8	303.9

The calculated hydrodynamic mass for vertical motions agrees very well with the experimental values for the ship on forward speed. For the damping coefficients the agreement at the lower relative water depths and higher frequencies is less satisfactory, which might be due to viscous influence. The same phenomena though less pronounced is found for the case of deep water [1, 2].

This applies also to the horizontal motions, sway and yaw, although the differences for damping are somewhat smaller than for the vertical motions.

A reasonable agreement is found for the distribution of mass and damping along the length of the shipmodel, except in those cases where wall effect could have influenced the experimental results, as discussed above.

Conclusions.

The results of this detailed comparison of measured and calculated mass and damping values for vertical and horizontal motions indicate that strip theory methods, using potential theory to determine

hydrodynamic mass and damping can be of value for the calculation of ship response due to waves in shallow water, at least for engineering purposes.

A limited number of model experiments to determine the amplitude response of heave and pitch in shallow water and the comparison with calculated motions confirm this conclusion to a certain extent for the vertical motions [5], see Figure 27 a+b.

Acknowledgement.

The authors are indebted to ing. A.P. de Zwaan who carried out the computerwork to calculate the hydrodynamic forces of the oscillating ship model in shallow water.

Nomenclature.

A_{wl}	waterplane area
a	added mass and added mass moment of inertia on speed, subscript for amplitude
B	beam
b	damping coefficient on speed
C_b	blockcoefficient
c	restoring force coefficient
d	cross-coupling coefficient for added mass
e	cross-coupling coefficient for damping
F	force exerted by oscillator
F_n	Froude number
g	restoring moment coefficient, acceleration due to gravity
h	water depth
I	mass moment of inertia
I_{wl}	longitudinal moment of inertia of waterplane
L	length of model
l	distance between oscillator legs ($l=1m$)
M	moment exerted by oscillator
m	added mass for zero speed
N	damping for zero speed
r	amplitude of oscillation
T	draught of model
t	time
V	forward speed of model
x, y, z	right hand coordinate system
y	sway displacement
z	heave displacement
ϵ	phase angle between force or moment and motion
θ	pitch angle
ρ	density of water
ψ	yaw angle
ω	circular frequency of oscillation
∇	volume of displacement of model
ζ	instantaneous wave elevation

Superscripts:

- * asterix for value of segment
- ' indication for sectional values of hydrodynamic coefficients

References.

1. Gerritsma, J., W. Beukelman "The Distribution of the Hydrodynamic Forces on a Heaving and Pitching Ship Model in Still Water", 5th Office of Naval Research Symposium 1964, Bergen, Norway
2. Gerritsma, J., W. Beukelman, Analysis of the Modified Strip Theory for the calculation of Ship Motions and Wave Bending Moments", International Shipbuilding Progress, 1967.

3. Keil, H., Die hydrodynamischen Kräfte bei der periodischen Bewegung zweidimensionaler Körper an der Oberfläche Gewässer, Bericht nr. 305, Institut für Schiffbau der Universität Hamburg, 1974.

4. Gerritsma, J., W. Beukelman and C.C. Glansdorp, The Effect of Beam on the Hydrodynamic Characteristics of Ship Hulls, 10th Office of Naval Research Symposium, 1974, Boston, U.S.A.

5. Van Doorn, J., Modelproeven en ware grootte metingen met m.s. "Smal Agt" (in Dutch) Report no. 530, Ship Hydromechanics Laboratory, Delft University of Technology (October 1981).

Appendix 1.

Experimental determination of mass and damping with a segmented model.

For the four modes of motions considered the hydrodynamic coefficients of the segments are determined after substitution of the in-phase and quadrature component of the measured sectional force into the equation of motion of the segment (2). In this way it can be shown that for:

Heave:

$$a_{zz}^* = \frac{c_a^* z_a - F_z^* \cos \epsilon_z^*}{z_a^2 \omega^2} - \rho \nabla^*$$

$$b_{zz}^* = \frac{F_z^* \sin \epsilon_z^*}{z_a \omega}$$

Pitch:

$$d_{z\theta}^* = \frac{g_{z\theta}^* \theta_a + F_\theta^* \cos \epsilon_\theta^*}{\theta_a \omega^2} - \rho \nabla^* x_i$$

$$e_{z\theta}^* = \frac{-F_\theta^* \sin \epsilon_\theta^*}{\theta_a \omega}$$

Sway:

$$a_{yy}^* = \frac{-F_y^* \cos \epsilon_y^*}{y_a \omega^2} - \rho \nabla^*$$

$$b_{yy}^* = \frac{F_y^* \sin \epsilon_y^*}{y_a \omega}$$

Yaw:

$$d_{y\psi}^* = \frac{F_\psi^* \cos \epsilon_\psi^*}{\omega^2 \psi_a} - \rho \nabla^* x_i$$

$$e_{y\psi}^* = \frac{-F_\psi^* \sin \epsilon_\psi^*}{\omega \psi_a}$$

where $\rho \nabla^* x_i$ is the mass moment of the segment which centre is located at a distance x_i from the centre of rotation. z_a, θ_a, y_a and ψ_a are the amplitudes of the related motions.

The coefficients of the segments divided by the length of the segment give the mean hydrodynamic cross-section coefficients. Assuming that the distribution of the cross-sectional values of the hydrodynamic coefficients are continuous curves these dis-

tributions can be determined from the seven mean cross-section values.

The hydrodynamic coefficients of the whole model are to be obtained as follows for:

Heave:	$a_{zz} = \Sigma a_{zz}^*$	Pitch:	$a_{\theta\theta} = \Sigma d_{z\theta}^* x_i$
	$b_{zz} = \Sigma b_{zz}^*$		$b_{\theta\theta} = \Sigma e_{z\theta}^* x_i$
	$d_{z\theta} = \Sigma d_{z\theta}^*$		$d_{\theta z} = \Sigma a_{zz}^* x_i$
	$e_{z\theta} = \Sigma e_{z\theta}^*$		$e_{\theta z} = \Sigma b_{zz}^* x_i$
Sway:	$a_{\psi\psi} = \Sigma a_{\psi\psi}^*$	Yaw:	$a_{\psi\psi} = \Sigma d_{\psi\psi}^* x_i$
	$b_{\psi\psi} = \Sigma b_{\psi\psi}^*$		$b_{\psi\psi} = \Sigma e_{\psi\psi}^* x_i$
	$d_{\psi\psi} = \Sigma d_{\psi\psi}^*$		$d_{\psi\psi} = \Sigma a_{\psi\psi}^* x_i$
	$e_{\psi\psi} = \Sigma e_{\psi\psi}^*$		$e_{\psi\psi} = \Sigma b_{\psi\psi}^* x_i$

Similar relations are used for the sectional values of the calculated coefficients as denoted in appendix 2.

Appendix 2.

Expressions according to version 1 and version 2 of the strip theory for the hydrodynamic mass-, damping- and cross coupling coefficients.

The expressions for the sectional values of the hydrodynamic coefficients are derived from appendix 1 in [4] and may be written for the motions considered as follows:

Heave:

$$a'_{zz} = m' + \left[\frac{V}{\omega^2} \frac{dN'}{dx} \right]$$

$$b'_{zz} = N' - V \frac{dm'}{dx}$$

$$d'_{z\theta} = m'x + \left[2 \right] \frac{V}{\omega^2} N' - \frac{V^2}{\omega^2} \frac{dm'}{dx} + \left[\frac{V}{\omega^2} \frac{dN'}{dx} x \right]$$

$$e'_{z\theta} = N'x - 2Vm' - V \frac{dm'}{dx} x - \left[\frac{V^2}{\omega^2} \frac{dN'}{dx} \right]$$

Pitch:

$$a'_{\theta\theta} = m'x^2 + 2 \frac{V}{\omega^2} N'x - \frac{V^2}{\omega^2} \frac{dm'}{dx} + \left[\frac{V}{\omega^2} \frac{dN'}{dx} x^2 \right]$$

$$b'_{\theta\theta} = N'x^2 - 2Vm'x - V \frac{dm'}{dx} x^2 - \left[\frac{V^2}{\omega^2} \frac{dN'}{dx} x \right]$$

$$d'_{\theta z} = m'x + \left[\frac{V}{\omega^2} \frac{dN'}{dx} x \right]$$

$$e'_{\theta z} = N'x - V \frac{dm'}{dx} x$$

Sway:

$$a'_{\psi\psi} = m' + \left[\frac{V}{\omega^2} \frac{dN'}{dx} \right]$$

$$b'_{\psi\psi} = N' - V \frac{dm'}{dx}$$

$$d'_{\psi\psi} = m'x + \left[2 \right] \frac{V}{\omega^2} N' - \frac{V^2}{\omega^2} \frac{dm'}{dx} + \left[\frac{V}{\omega^2} \frac{dN'}{dx} x \right]$$

$$e'_{\psi\psi} = N'x - 2Vm' - V \frac{dm'}{dx} x - \left[\frac{V^2}{\omega^2} \frac{dN'}{dx} \right]$$

Yaw:

$$a'_{\psi\psi} = m'x^2 + 2 \frac{V}{\omega^2} N'x - \frac{V^2}{\omega^2} \frac{dm'}{dx} x + \left[\frac{V}{\omega^2} \frac{dN'}{dx} x \right]$$

$$b'_{\psi\psi} = N'x^2 - 2Vm'x - V \frac{dm'}{dx} x^2 - \left[\frac{V^2}{\omega^2} \frac{dN'}{dx} x \right]$$

$$d'_{\psi\psi} = m'x + \left[\frac{V}{\omega^2} \frac{dN'}{dx} x \right]$$

$$e'_{\psi\psi} = N'x - V \frac{dm'}{dx} x$$

in which:

m' = sectional damping	} for zero speed
N' = sectional mass	
V = forward speed	
ω = frequency of oscillation	
a' = sectional added mass	} on speed
b' = sectional damping	
d' = sectional mass coupling coefficient	
e' = sectional damping coupling coefficient	
x = longitudinal	} direction
Y = sway	
z = heave	
θ = pitch	
ψ = yaw	

Version 1 = coefficients excluding terms between brackets

Version 2 = coefficients including terms between brackets

From the expressions for the sectional coefficients the following relations may be derived:

$a'_{\theta\theta} = d'_{z\theta} x$	$a'_{\psi\psi} = d'_{\psi\psi} x$
$b'_{\theta\theta} = e'_{z\theta} x$	$b'_{\psi\psi} = e'_{\psi\psi} x$
$d'_{\theta z} = a'_{zz} x$	$d'_{\psi Y} = a'_{\psi Y} x$
$e'_{\theta z} = b'_{zz} x$	$e'_{\psi Y} = b'_{\psi Y} x$

In appendix 1 the same relations are used for the measured values to obtain the not directly measured coefficients.

The values of the hydrodynamic mass-, damping- and cross coupling coefficients for the whole model are obtained by integration of the sectional values over the model-length.

W. Beukelman
J. Gerritsma
Ship Hydromechanics Laboratory
Delft University of Technology
Delft
The Netherlands

РАСПРЕДЕЛЕНИЕ ГИДРОДИНАМИЧЕСКИХ МАСС И ДЕМПФИРОВАНИЯ ОСЦИЛЛИРУЮЩИХ СУДОПОДОБНЫХ ФОРМ НА МЕЛКОВОДЬЕ

Длительное применение теории плоских сечений в расчетах качки судна на глубокой воде показало, что она дает удовлетворительные для практики результаты, точность которых однако, зависит от точности определения коэффициентов присоединенных масс и демпфирования. В условиях мелководья корректность этой теории ставится под вопрос ввиду ожидаемого влияния вязкости и особен-

ностей обтекания оконечностей. Для исследования влияния этих эффектов на возможность применения теории плоских сечений и для случая мелкой воды, сделано сравнение распределения коэффициентов присоединенных масс и демпфирования по длине судна, определенных экспериментально в процессе вынужденных колебаний разрезной модели серии 60 на мелководье, а также вычисленных по теории плоских сечений Кейля с учетом конечной глубины. Вязкость, посадка и ходовой дифферент не учитывались. Условия испытания включали изменения относительной глубины h/T , амплитуд и частот колебаний, а также скорости судна.

Результаты подробного сравнения измеренных и вычисленных гидродинамических коэффициентов свидетельствуют о применимости потенциальной теории в практических инженерных расчетах как поперечных, так и продольных видов качки на мелководье. В то же время, при низких частотах и малых скоростях хода отмечено значительное расхождение, что объясняется влиянием стенки бассейна и особенностей волнообразования.

В.Бекелман
Дж.Герритсма
Дельфтский технологический Университет
Дельфт
Нидерланды

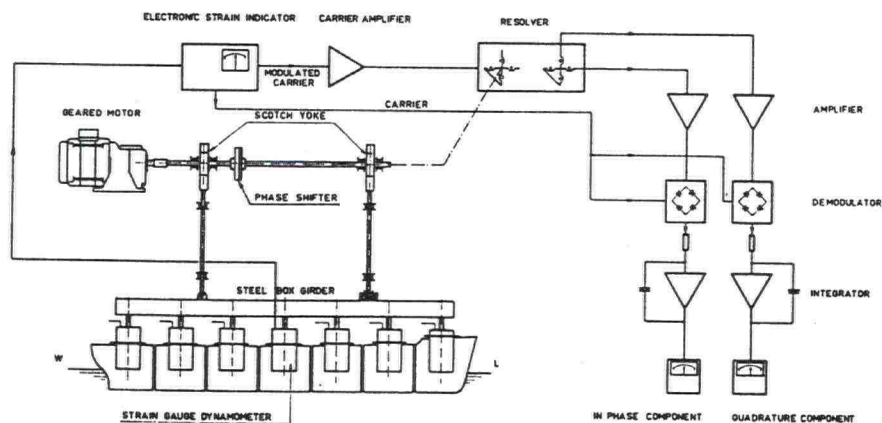


Figure 1. PRINCIPLE OF MECHANICAL OSCILLATOR AND ELECTRONIC CIRCUIT

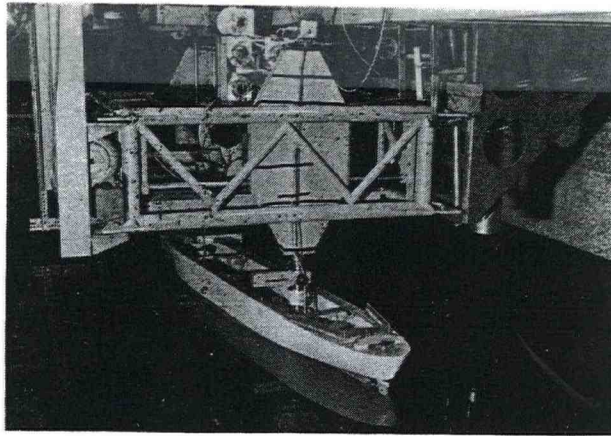


Figure 2: Horizontal oscillator.

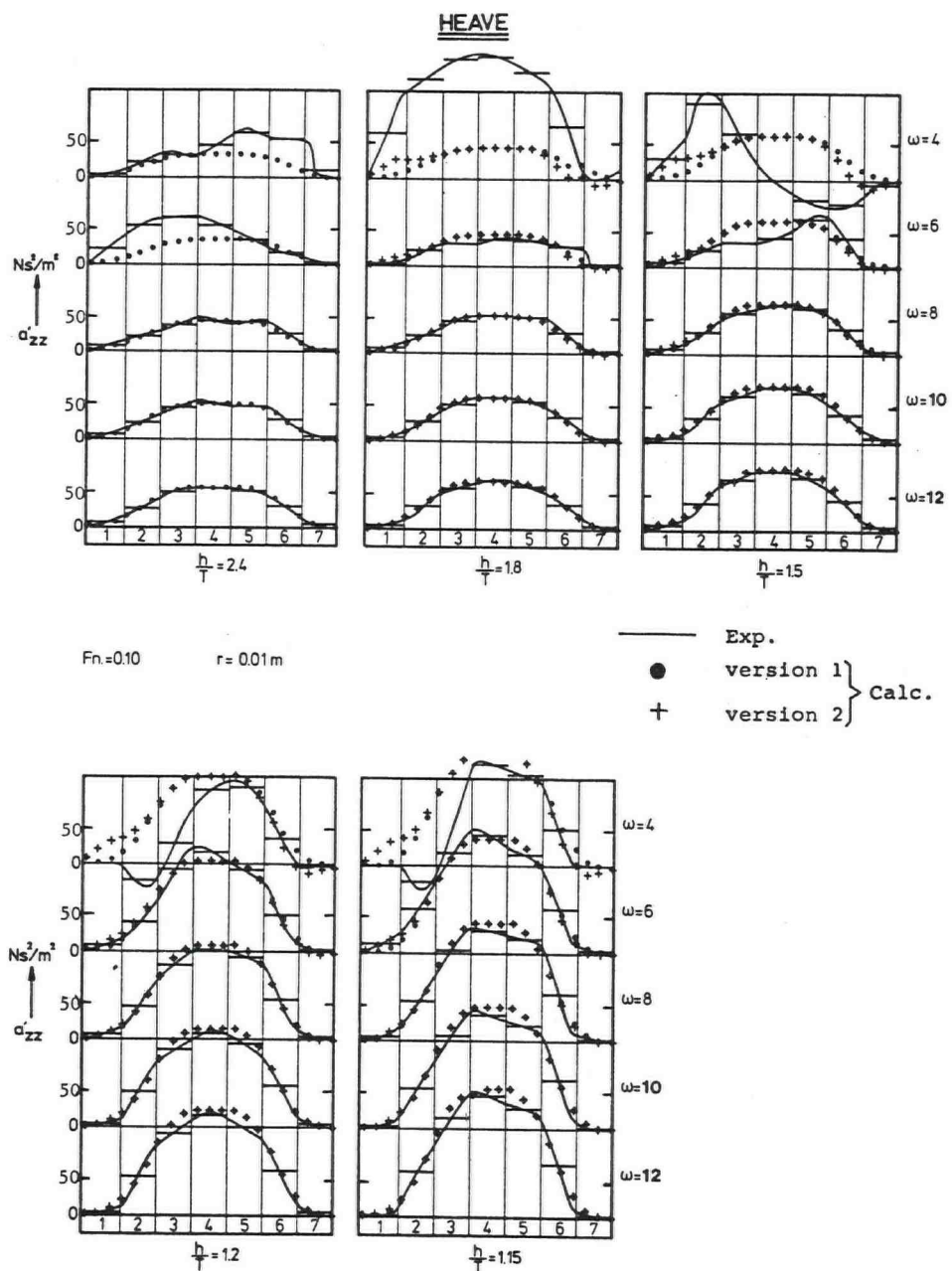
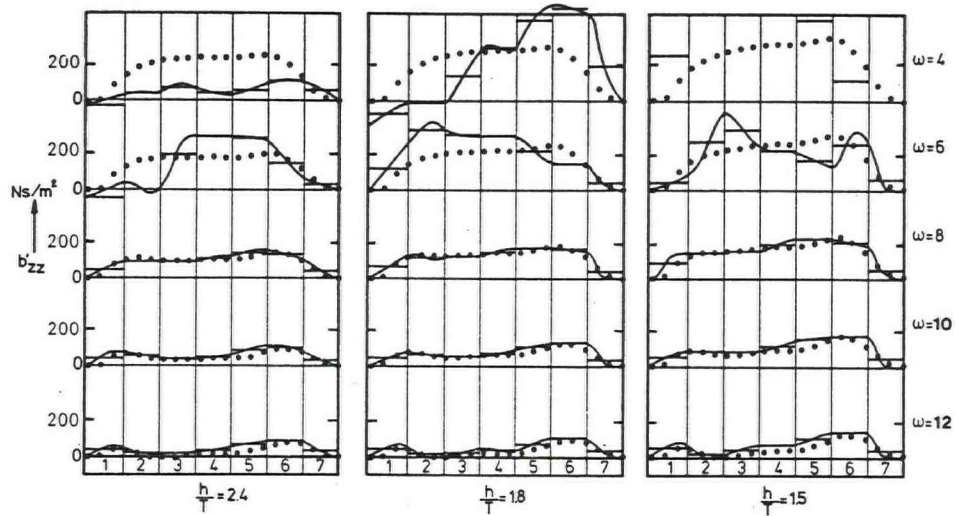


Fig.3: Comparison of experimental and calculated distribution of a_{zz} for five waterdepth-draught ratios. $Fn=0.10$.

HEAVE



$F_n = 0.10$ $r = 0.01m$

— Exp.
 ● version 1 } Calc.
 + version 2 }

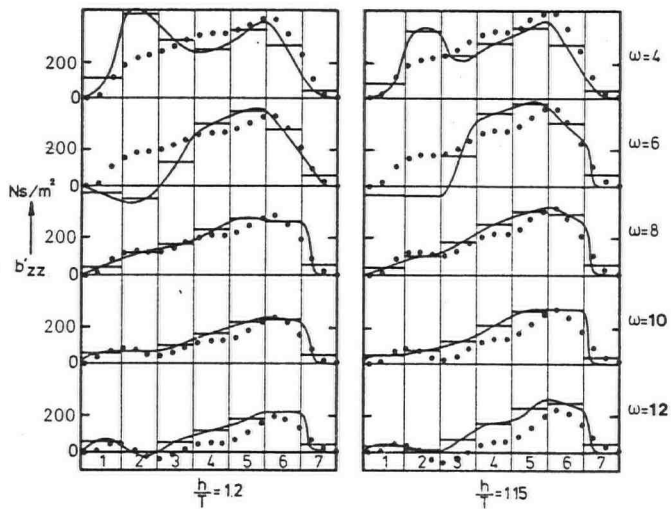


Fig.4: Comparison of experimental and calculated distribution of b_{zz} for five waterdepth-draught ratios. $F_n = 0.10$.

HEAVE

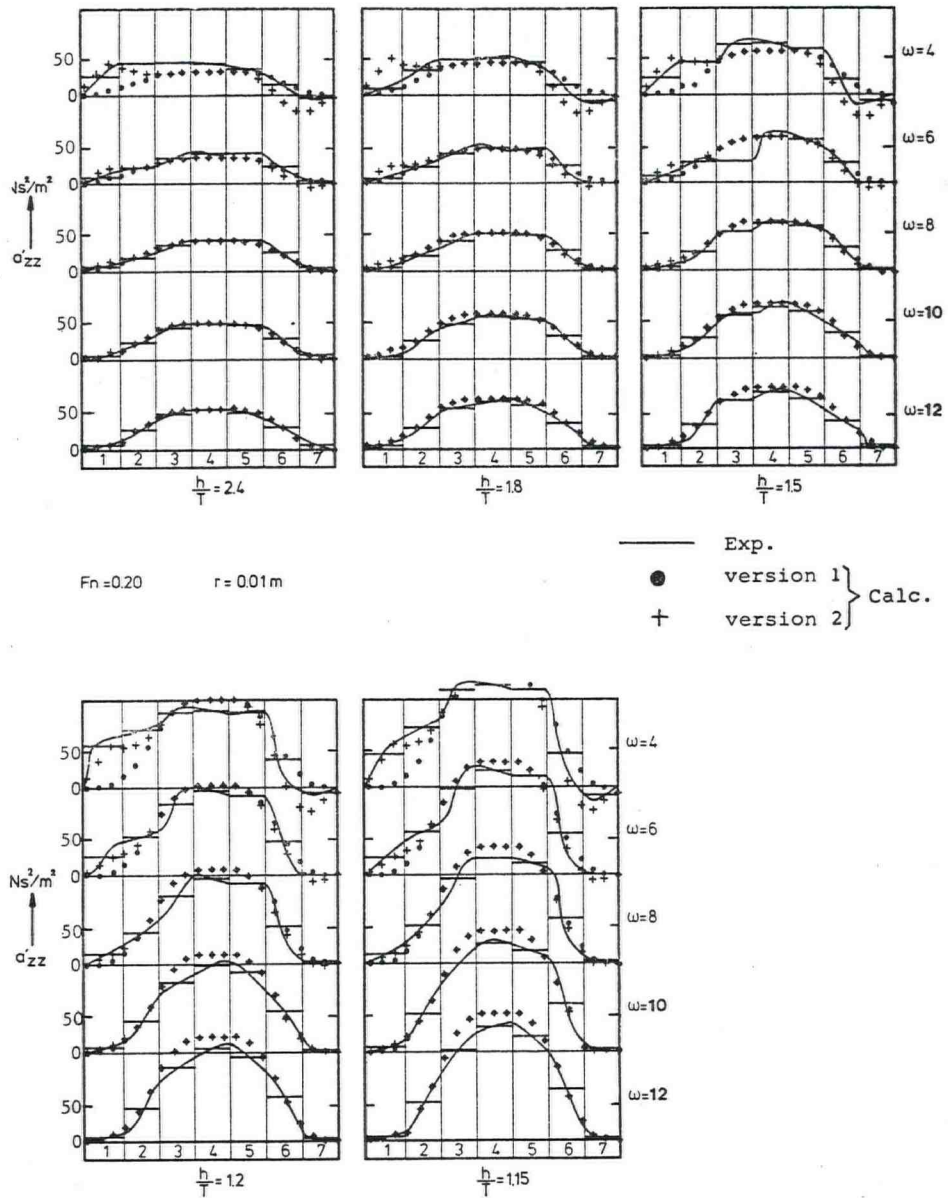


Fig.5: Comparison of experimental and calculated distribution of a_{zz} for five waterdepth-draught ratios. $F_n=0.20$.

HEAVE

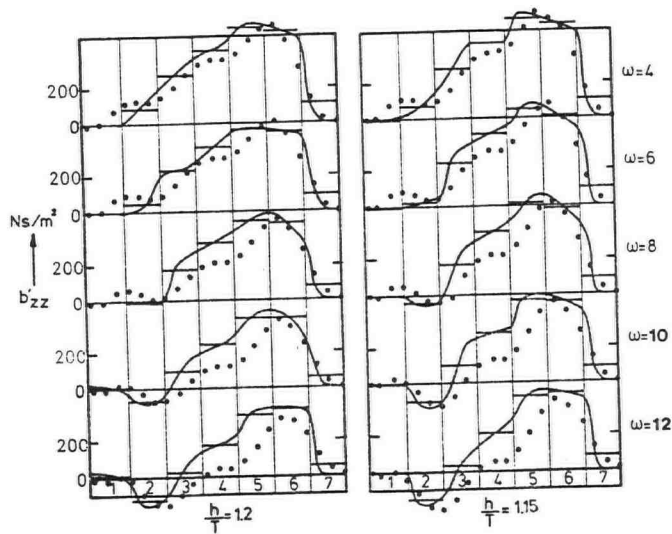
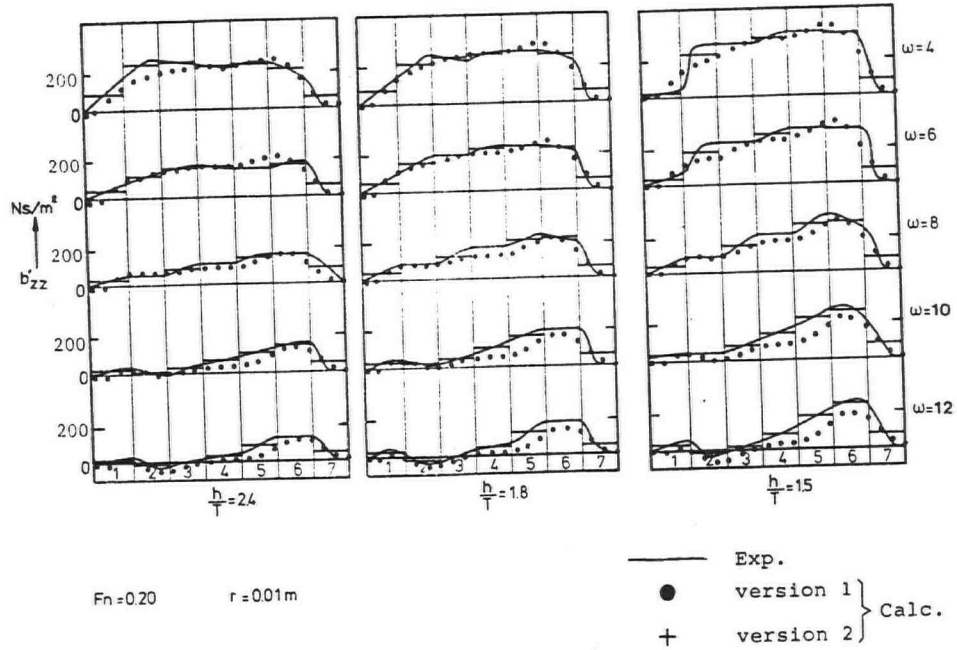


Fig.6: Comparison of experimental and calculated distribution of b_{zz} for five waterdepth-draught ratios. $F_n = 0.20$.

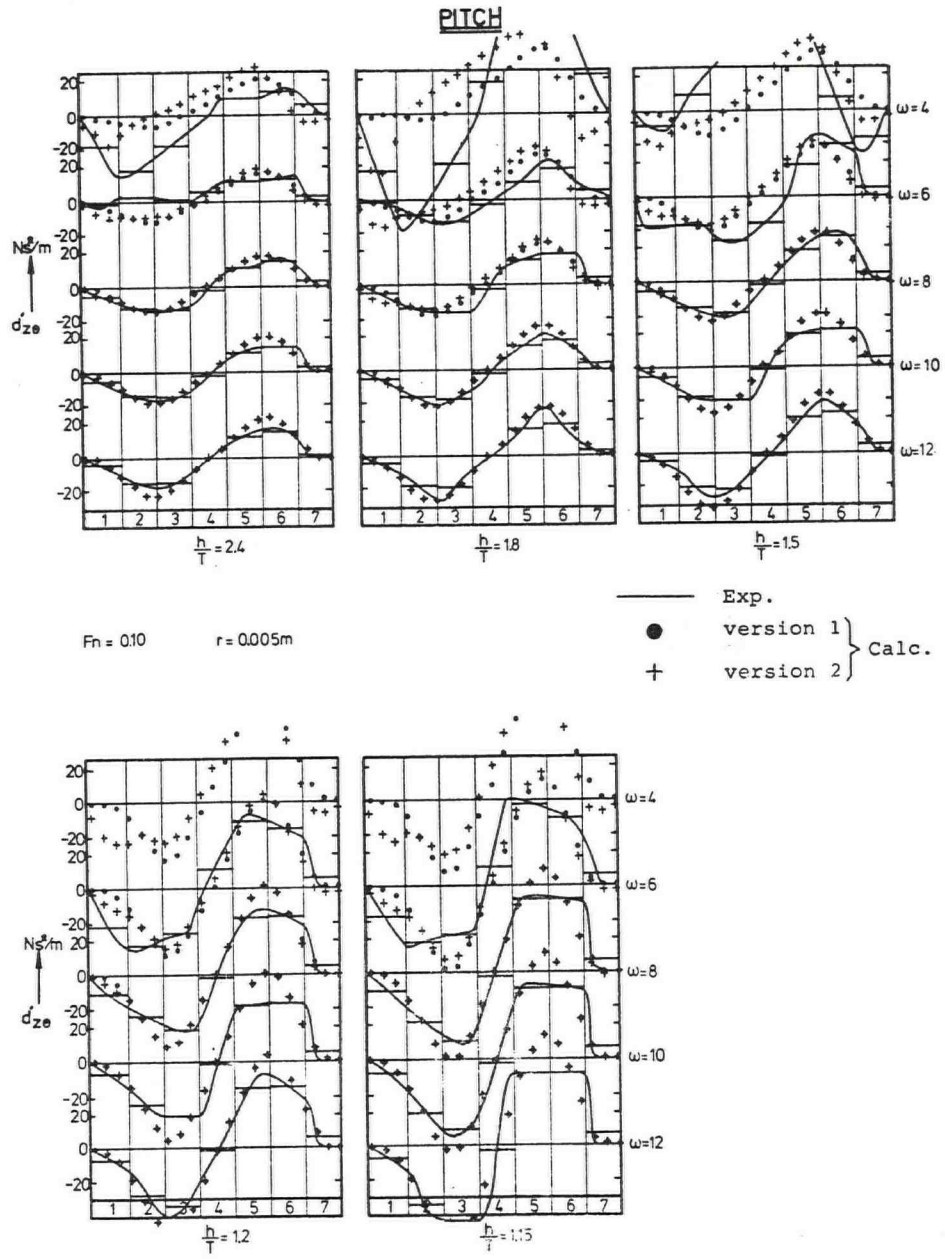
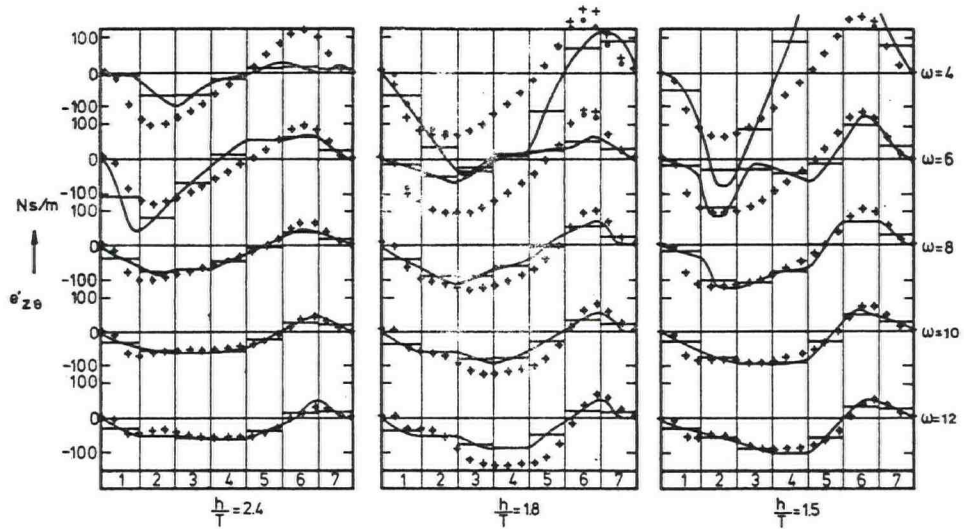


Fig.7: Comparison of experimental and calculated distribution of $d_{z\theta}$ for five waterdepth-draught ratios. $F_n=0.10$.

PITCH



$Fn = 0.10$ $r = 0.005 \text{ m}$

— Exp.
 ● version 1 } Calc.
 + version 2 }

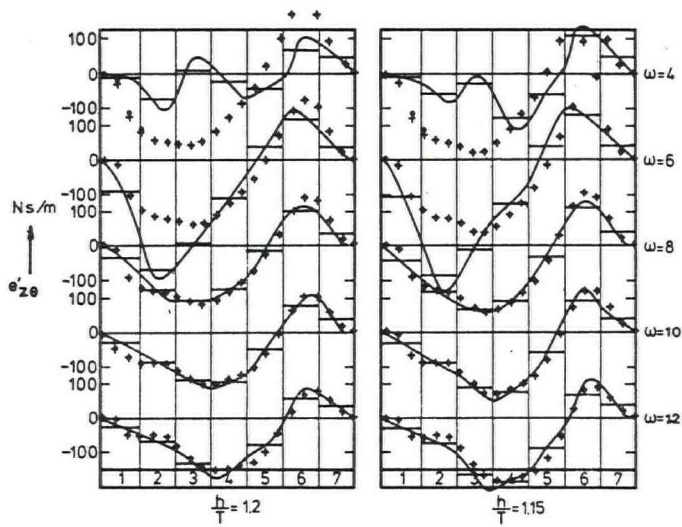
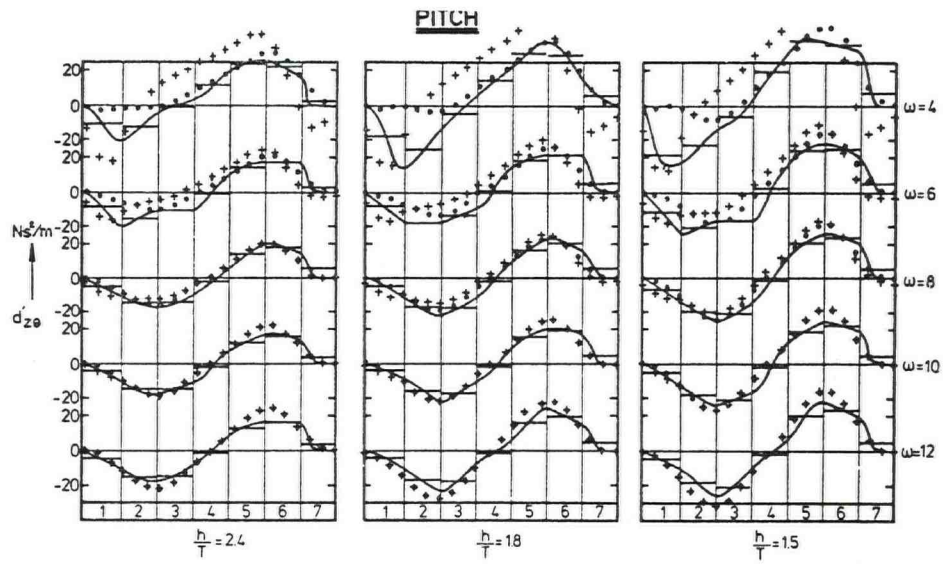


Fig.8: Comparison of experimental and calculated distribution of $e_{z\theta}$ for five waterdepth-draught ratios. $Fn=0.10$.



$Fn = 0.20$ $r = 0.005m$

— Exp.
 ● version 1 } Calc.
 + version 2 }

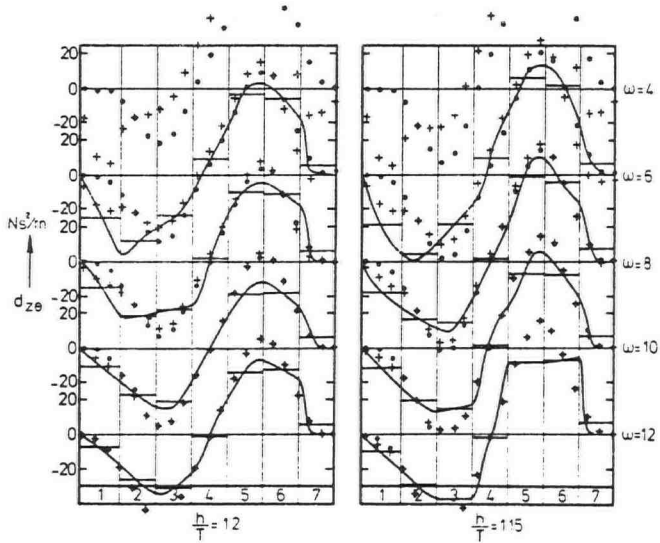


Fig.9: Comparison of experimental and calculated distribution of d_{z0} for five waterdepth-draught ratios. $Fn = 0.20$.

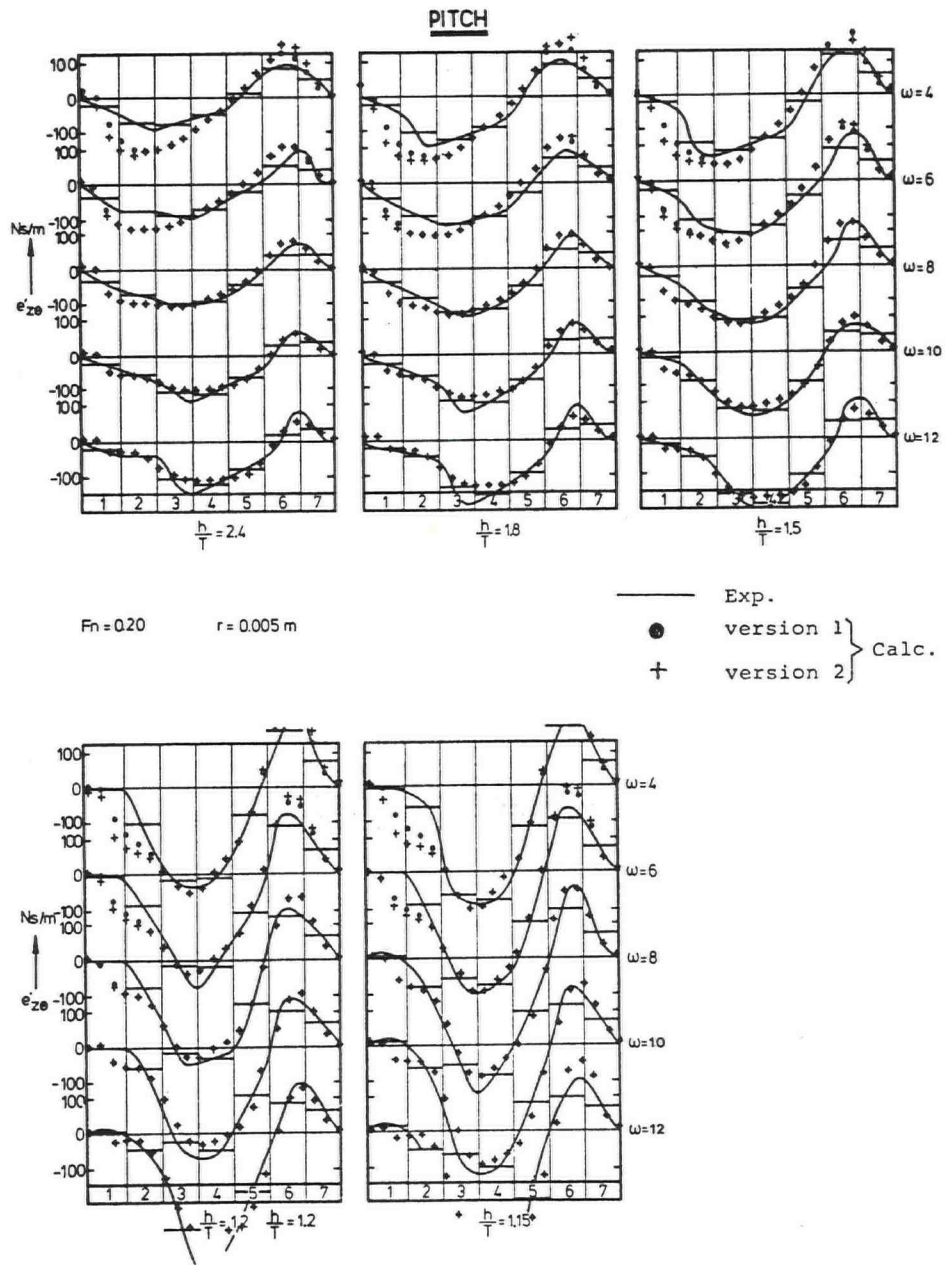
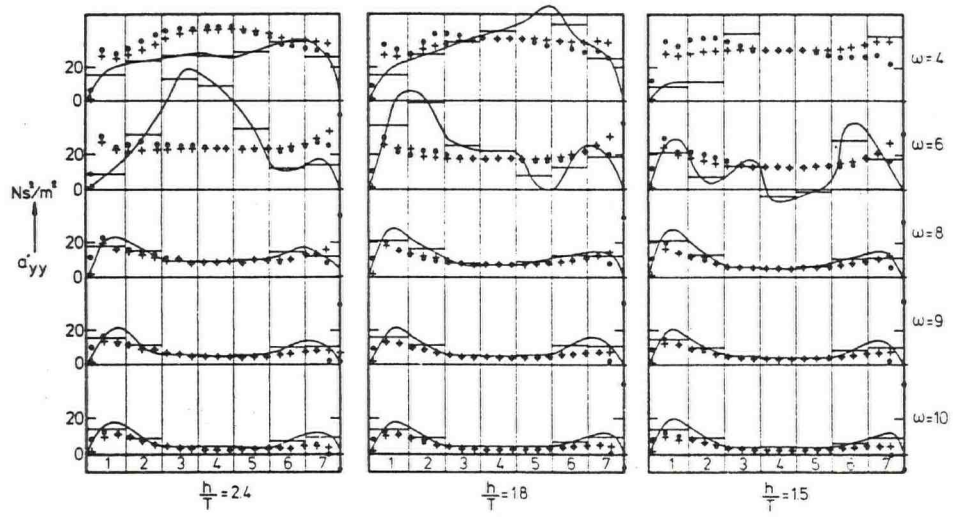


Fig.10: Comparison of experimental and calculated distribution of $e_{z,\theta}$ for five waterdepth-draught ratios. $F_n=0.20$

SWAY



$Fn=0.10$ $r=0.01m$

— Exp.
 ● version 1 } Calc.
 + version 2 }

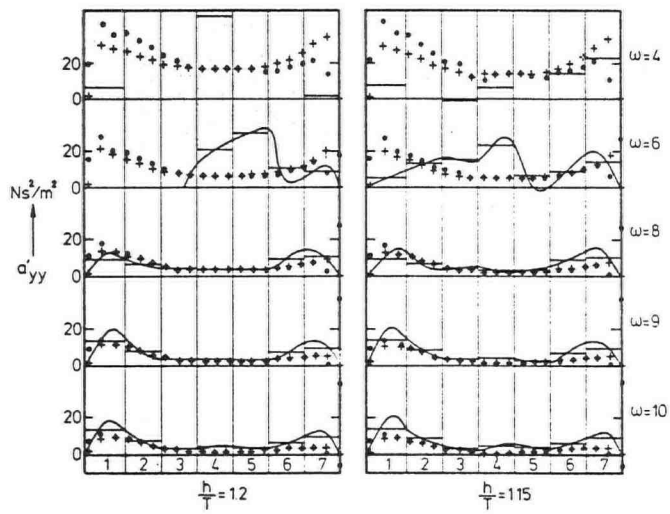


Fig.11: Comparison of experimental and calculated distribution of a_{yy} for five waterdepth-draught ratios. $Fn.=0.10$.

SWAY

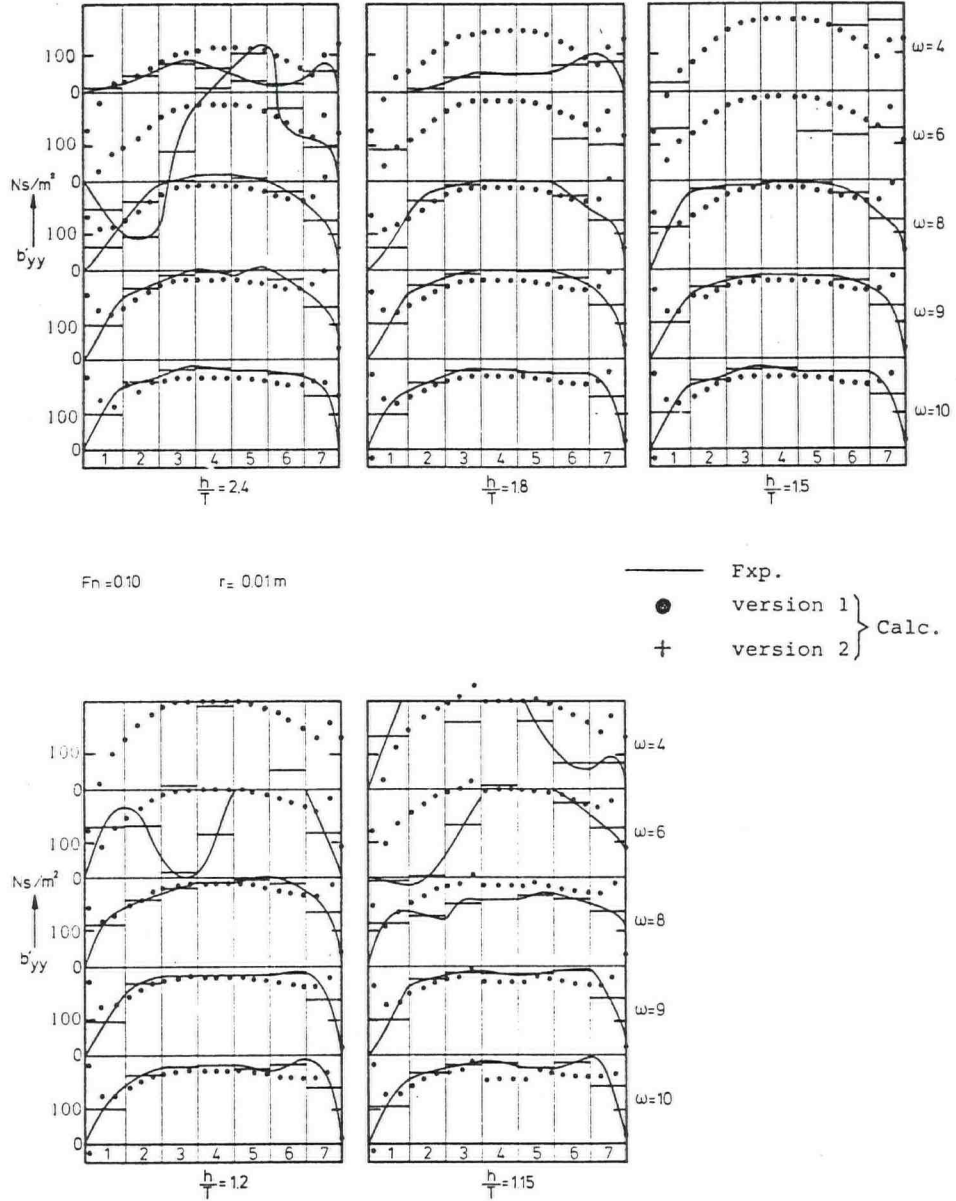
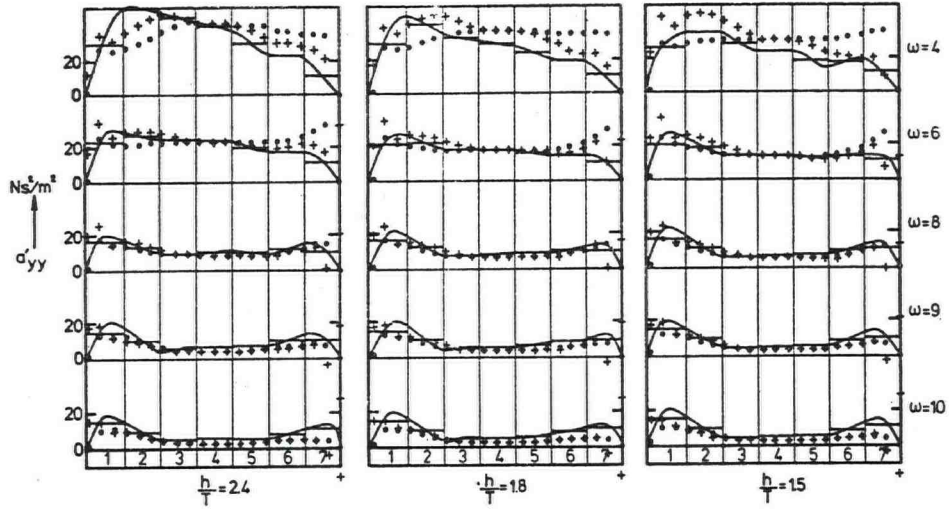


Fig.12: Comparison of experimental and calculated distribution of b'_{yy} for five waterdepth-draught ratios. $F_n = 0.10$.

SWAY



$Fn=0.20$ $r=0.01m$

— Exp.
 ● version 1 } Calc.
 + version 2 }

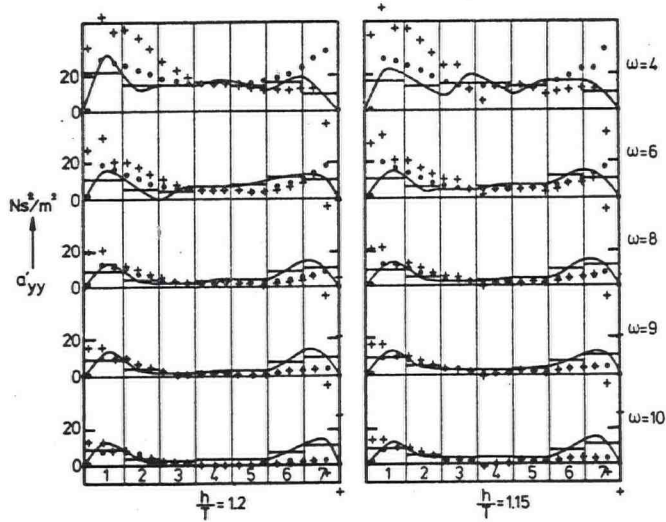
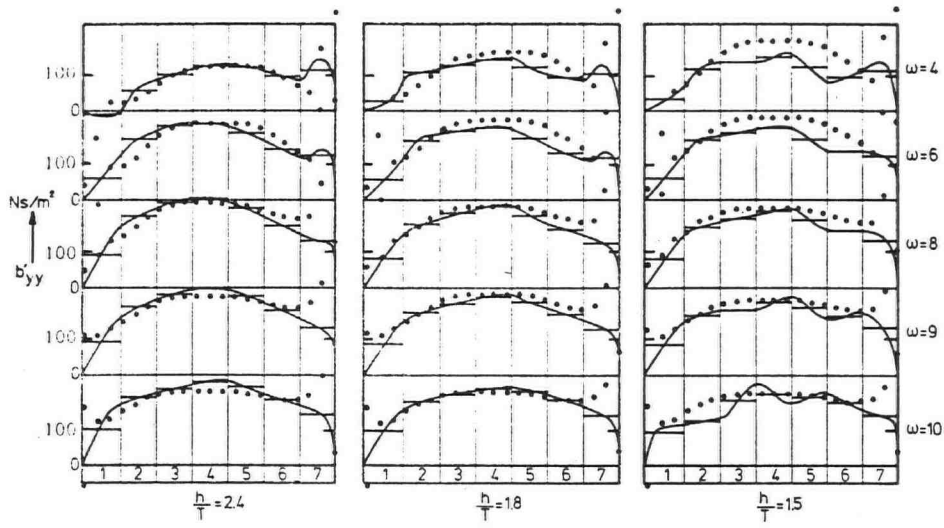


Fig.13: Comparison of experimental and calculated distribution of a_{yy} for five waterdepth-draught ratios. $Fn.=0.20$.

SWAY



$Fn=0.20$ $r=0.01m$

— Exp.
 ● version 1 } Calc.
 + version 2 }

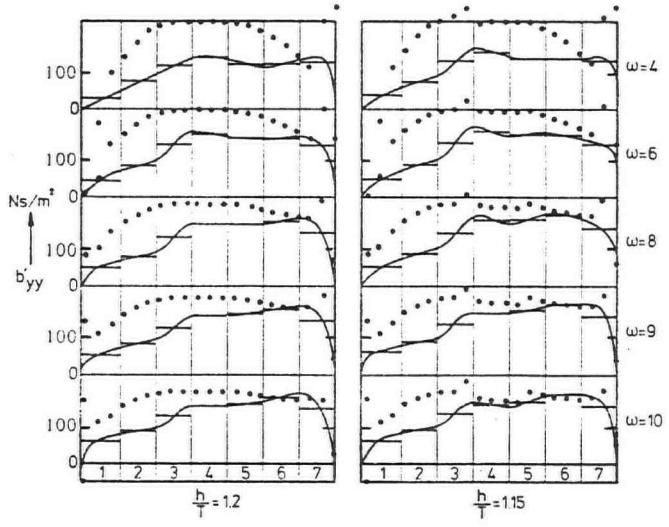
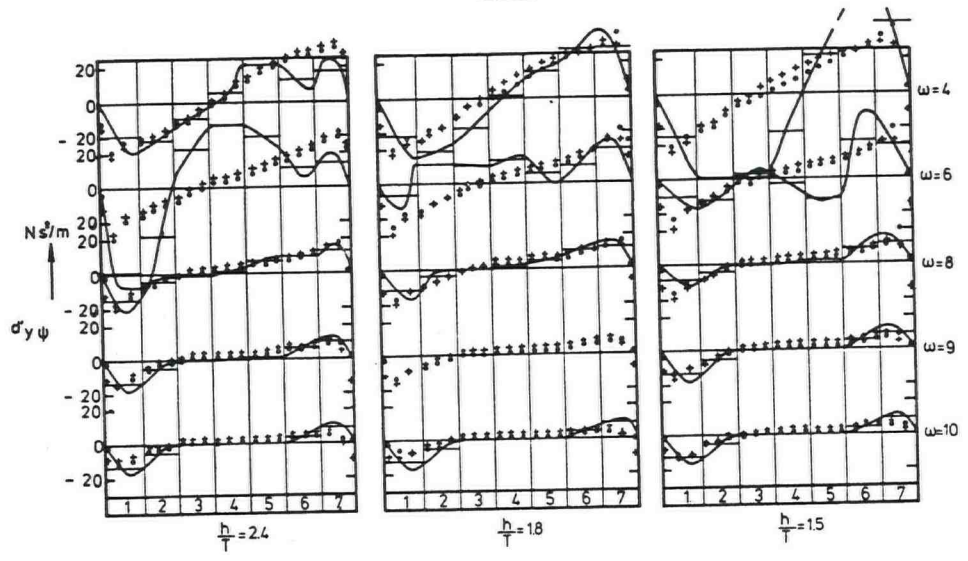


Fig.14: Comparison of experimental and calculated distribution of b'_{yy} for five waterdepth-draught ratios. $Fn=0.20$.

YAW



$Fn = 0.10$ $r = 0.01m$

— Exp.
 ● version 1 } Calc.
 + version 2 }

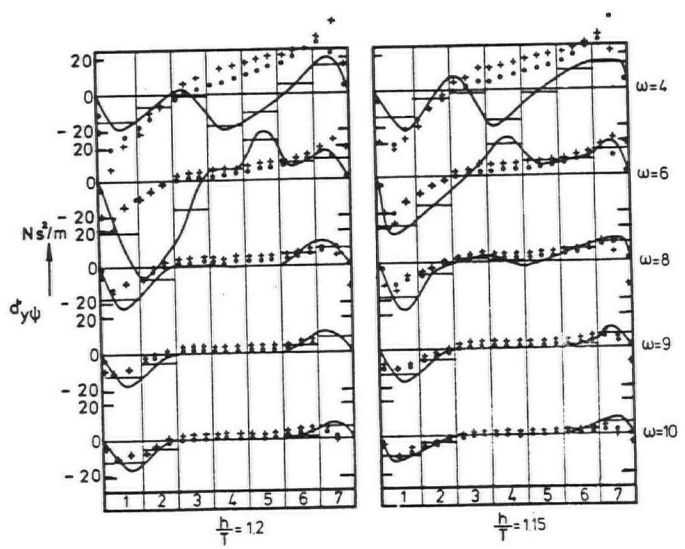


Fig.15: Comparison of experimental and calculated distribution of $d_{y\psi}$ for five waterdepth-draught ratios. $Fn.=0.10$.

YAW

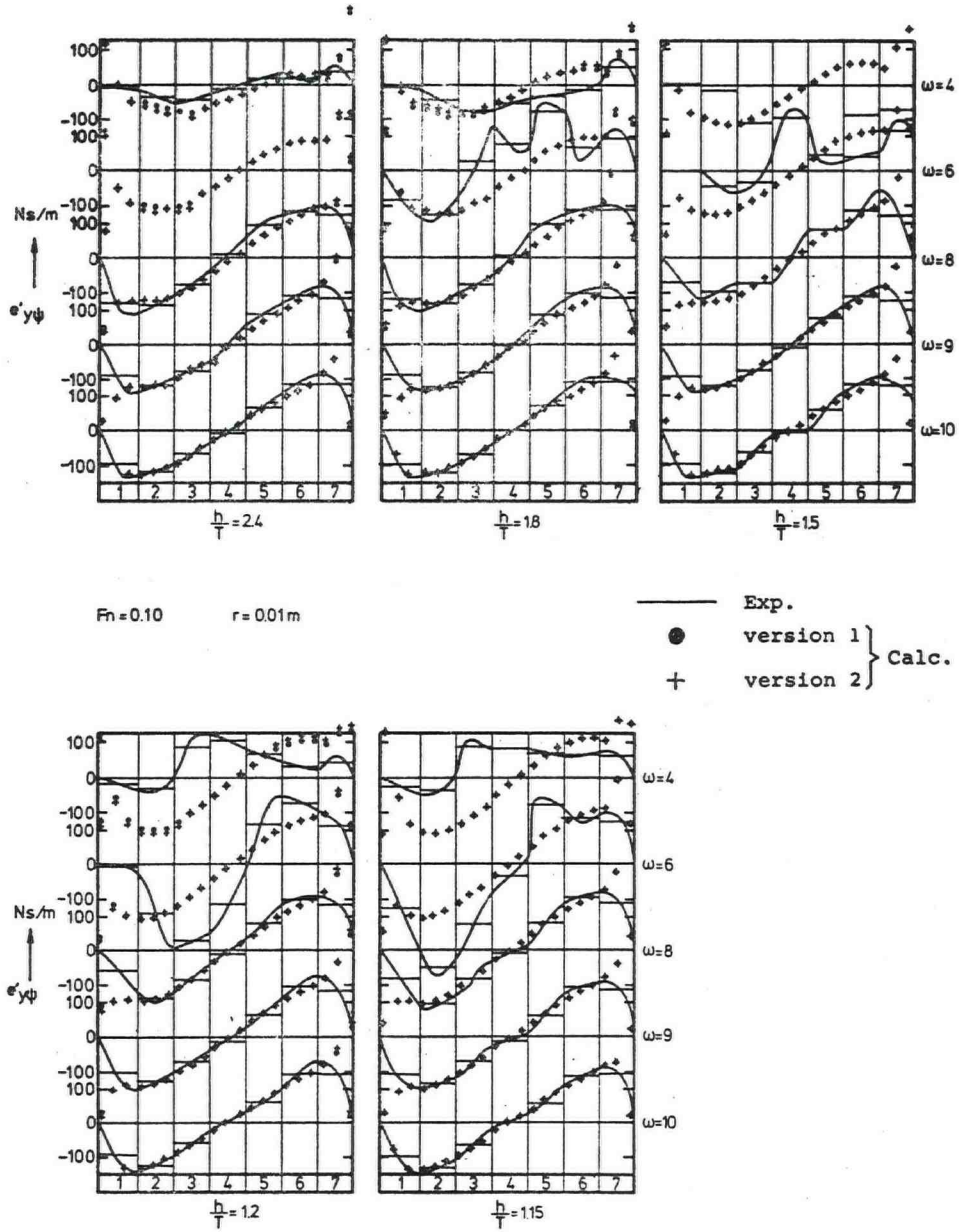
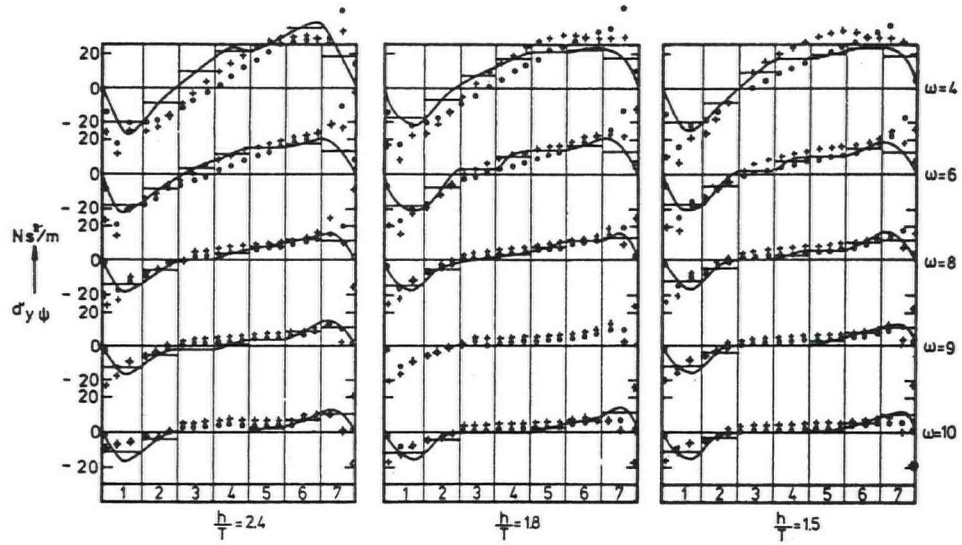


Fig.16: Comparison of experimental and calculated distribution of $e_{y\psi}$ for five waterdepth-draught ratios. $Fn=0.10$.

YAW



$Fn = 0.20$ $r = 0.01m$

— Exp.
 ● version 1 } Calc.
 + version 2 }

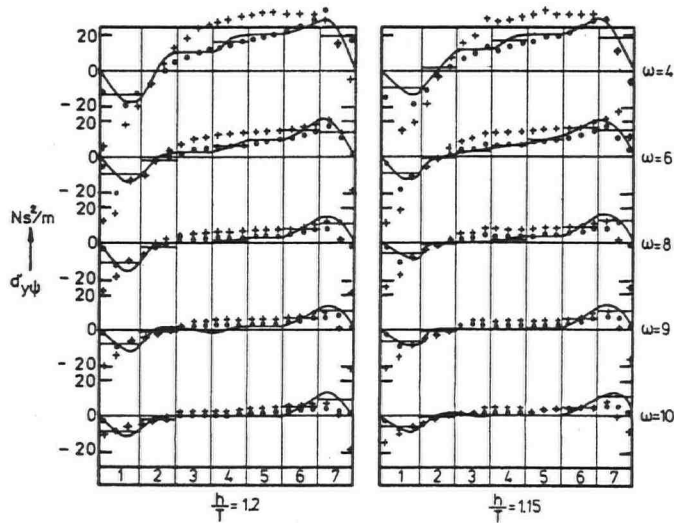


Fig.17: Comparison of experimental and calculated distribution of $d_{y\psi}$ for five waterdepth-draught ratios. $Fn=0.20$.

YAW

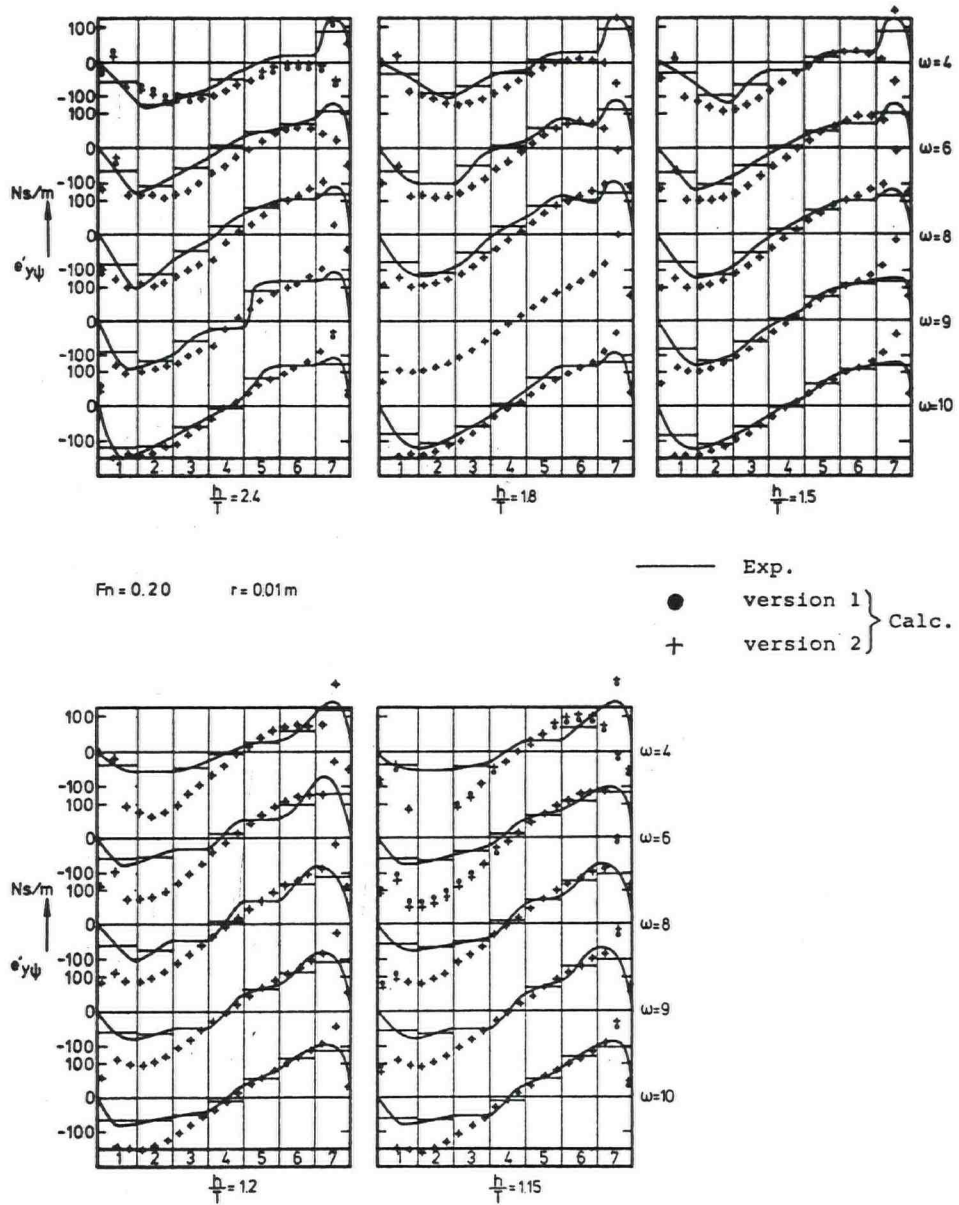


Fig.18: Comparison of experimental and calculated distribution of $e_{y\psi}$ for five waterdepth-draught ratios. $Fn=0.20$.

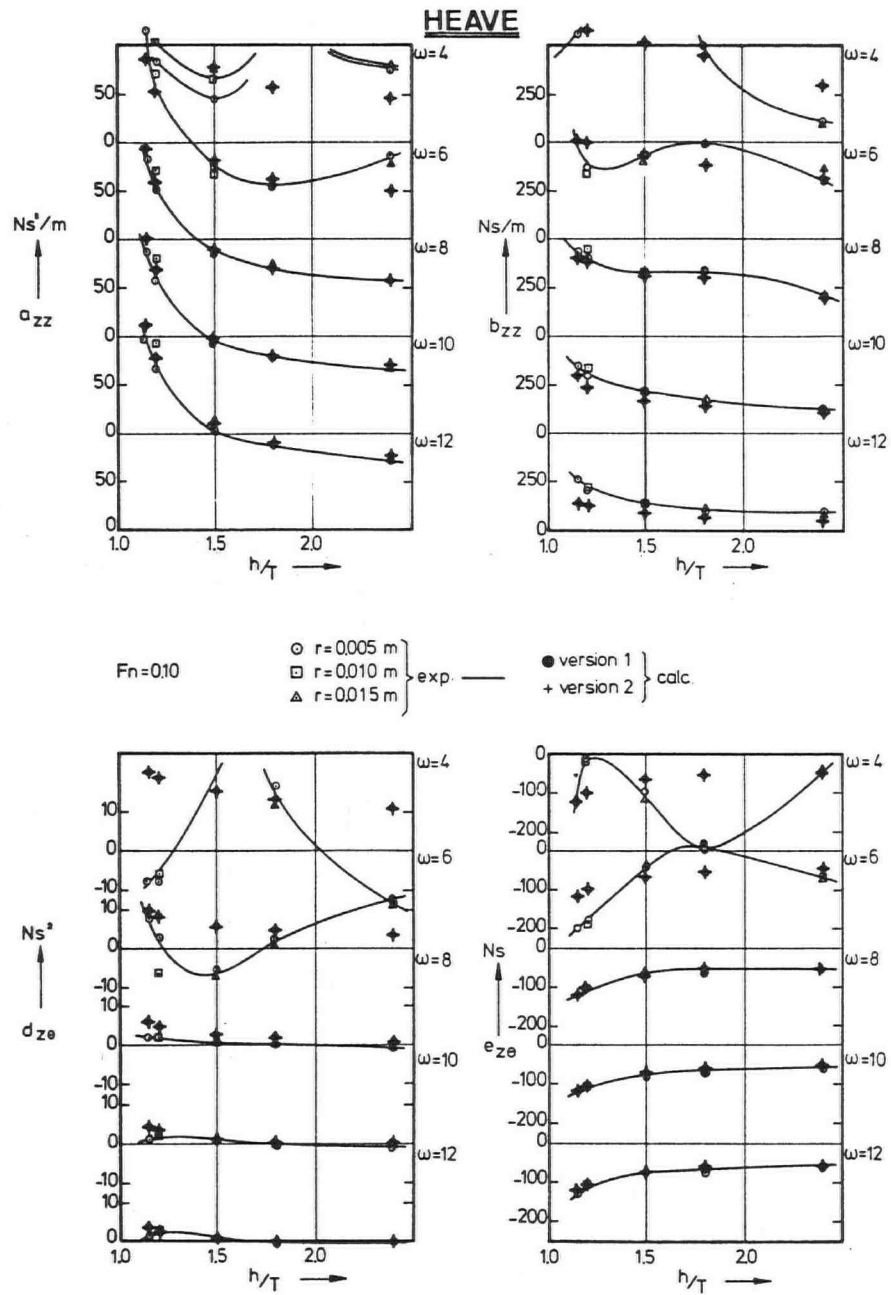


Fig.19: Comparison of experimental and calculated coefficients for heave as a function of waterdepth-draught ratio. $F_n = 0.10$.

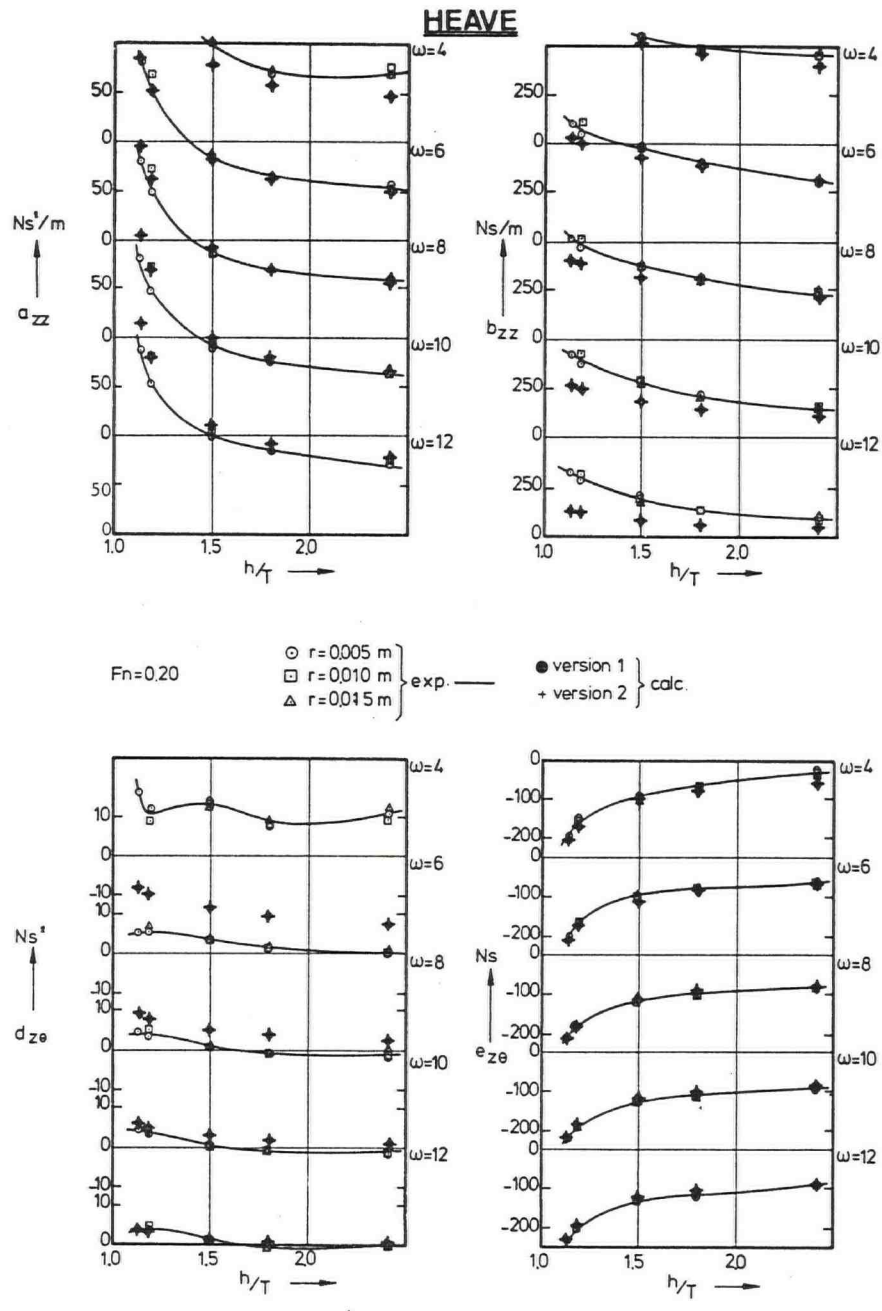


Fig.20: Comparison of experimental and calculated coefficients for heave as a function of waterdepth-draught ratio. $F_n=0.20$.

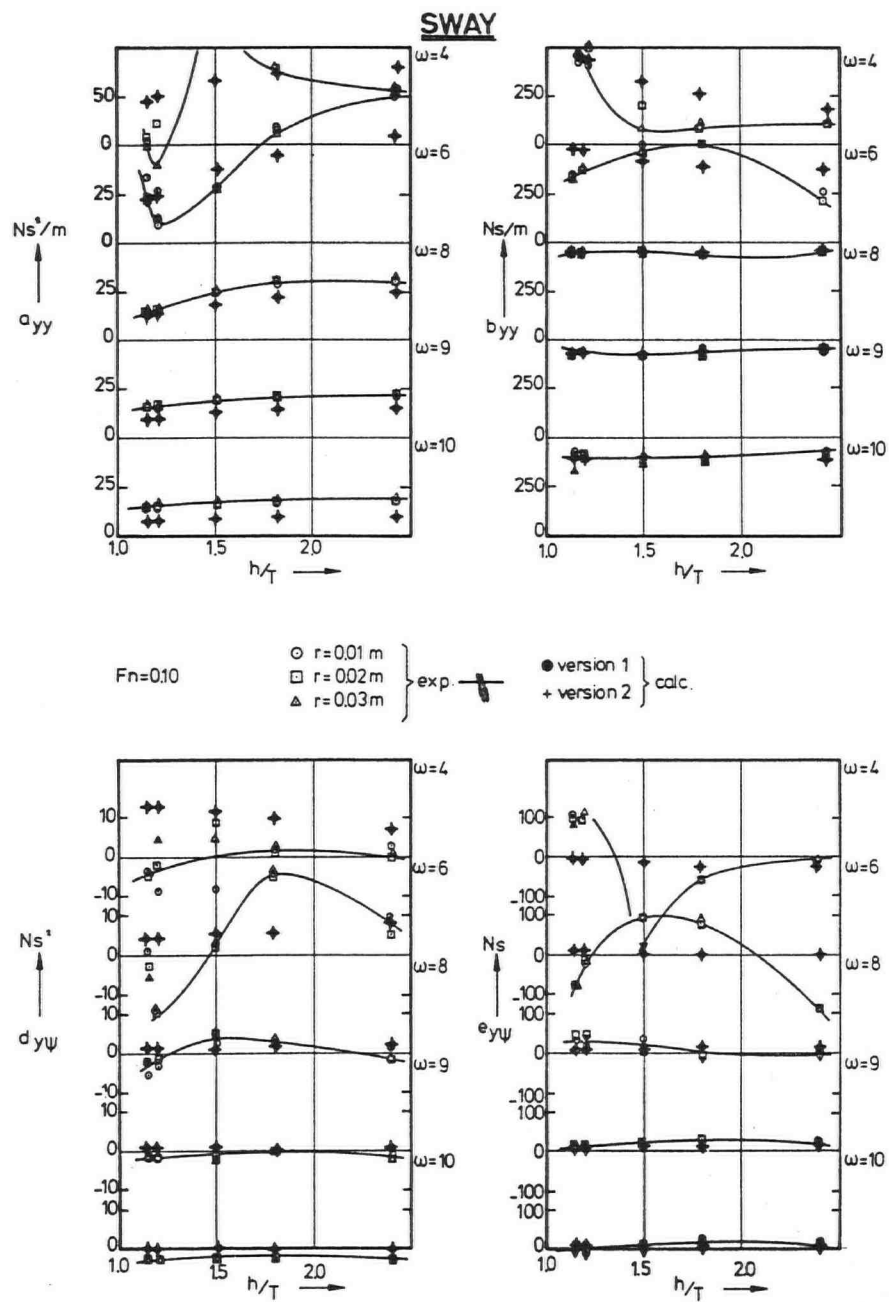


Fig.21: Comparison of experimental and calculated coefficients for sway as a function of waterdepth-draught ratio. $F_n=0.10$.

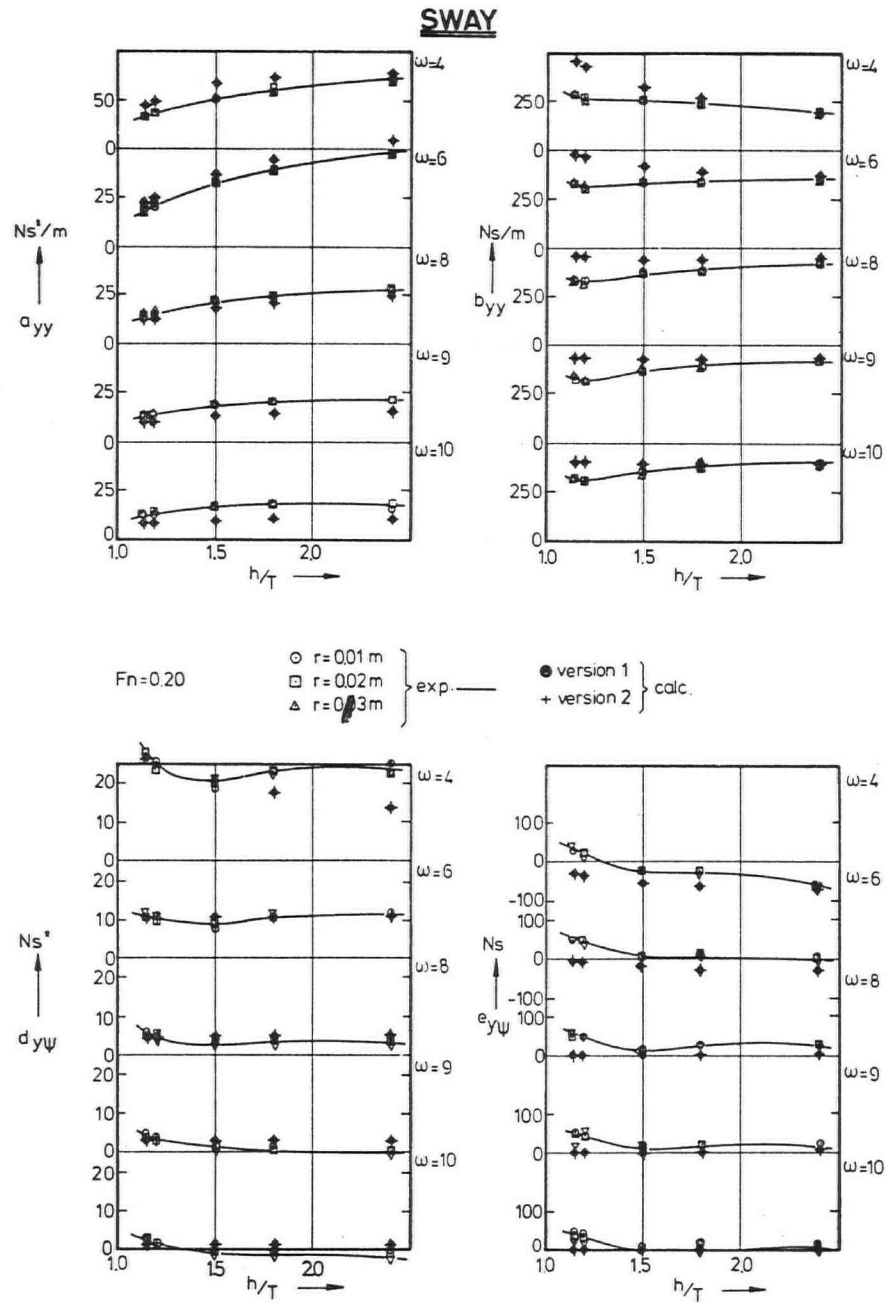


Fig.22: Comparison of experimental and calculated coefficients for sway as a function of waterdepth-draught ratio. $Fn=0.20$

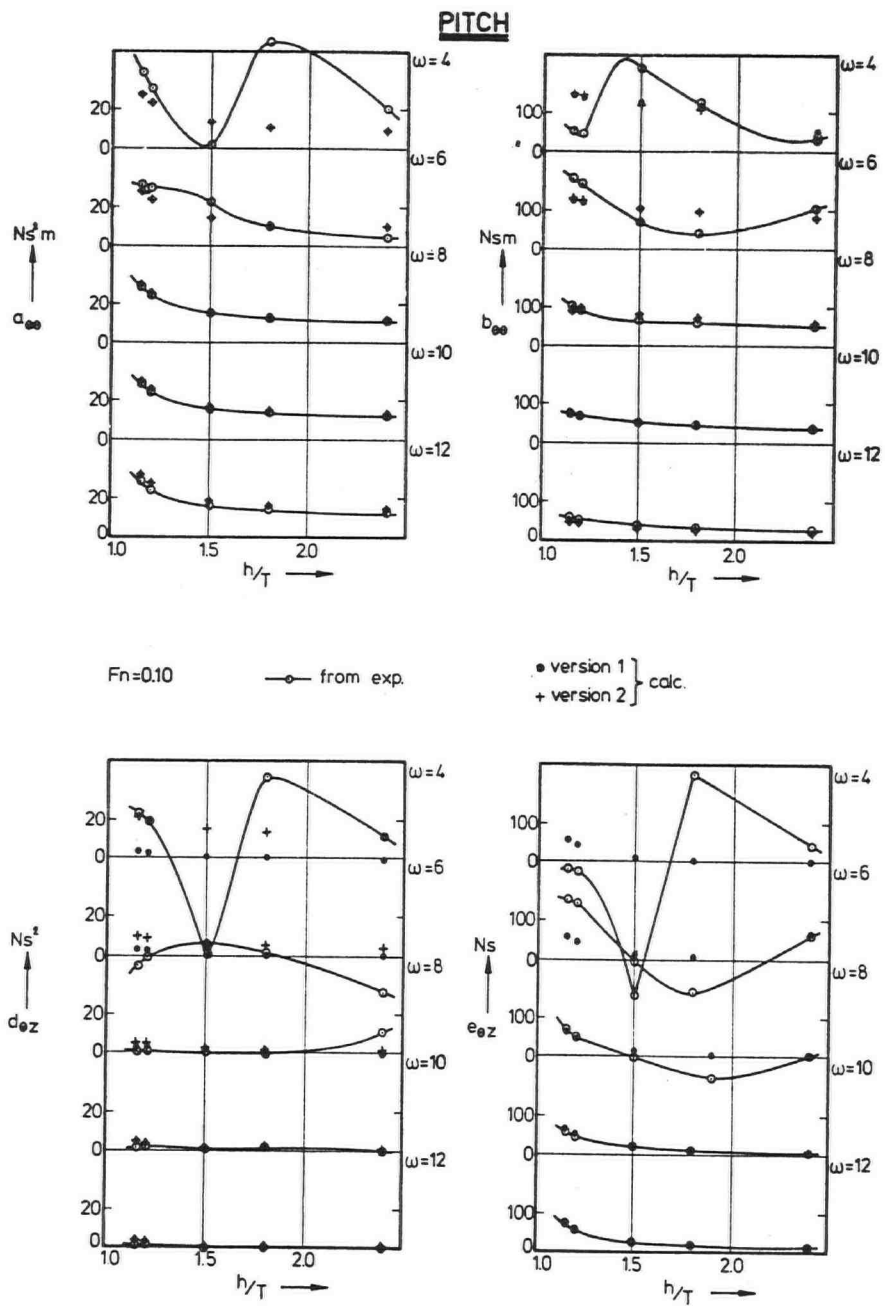


Fig.23: Comparison of experimental and calculated coefficients for pitch as a function of waterdepth-draught ratio. $Fn=0.10$

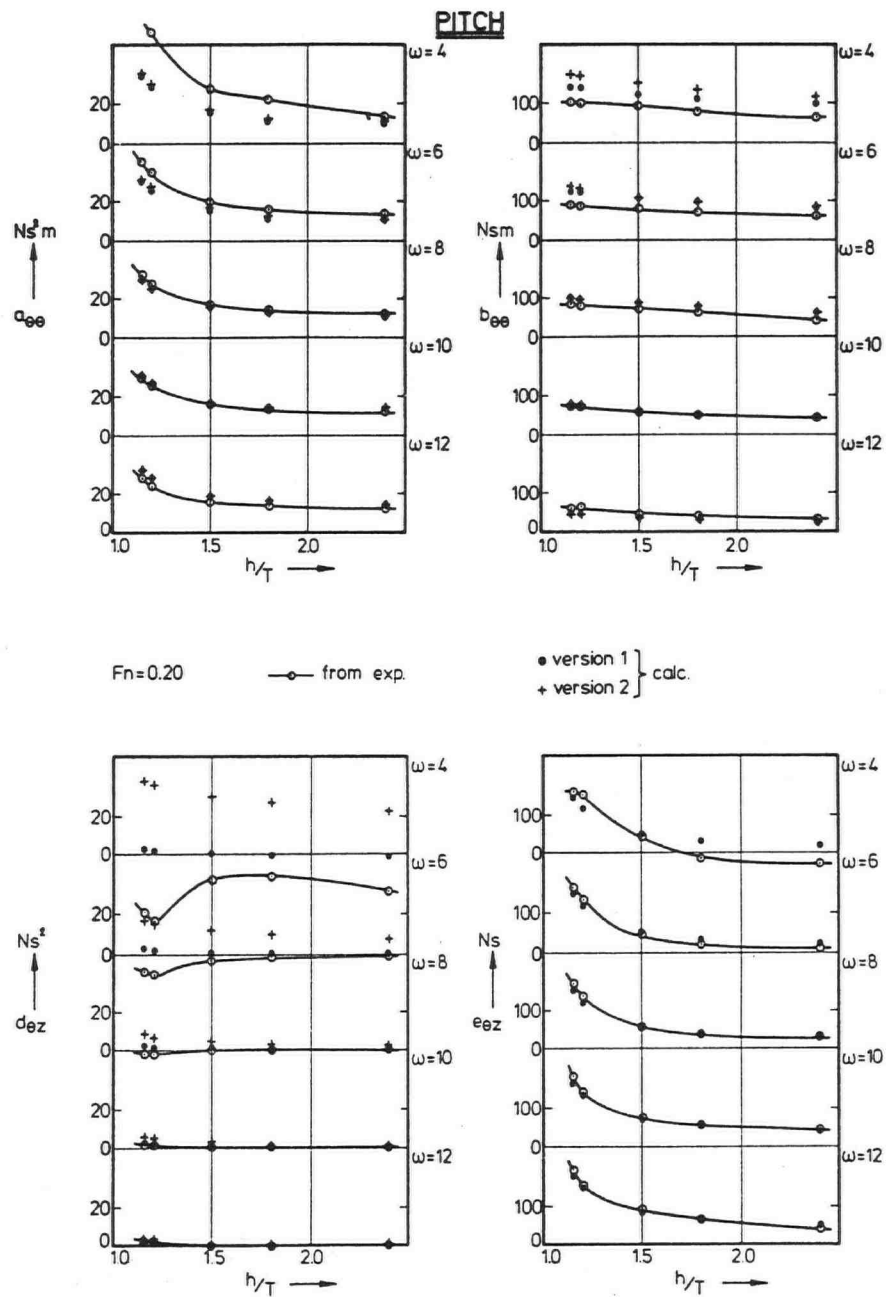


Fig.24: Comparison of experimental and calculated coefficients for pitch as a function of waterdepth-draught ratio. $Fn=0$.

YAW

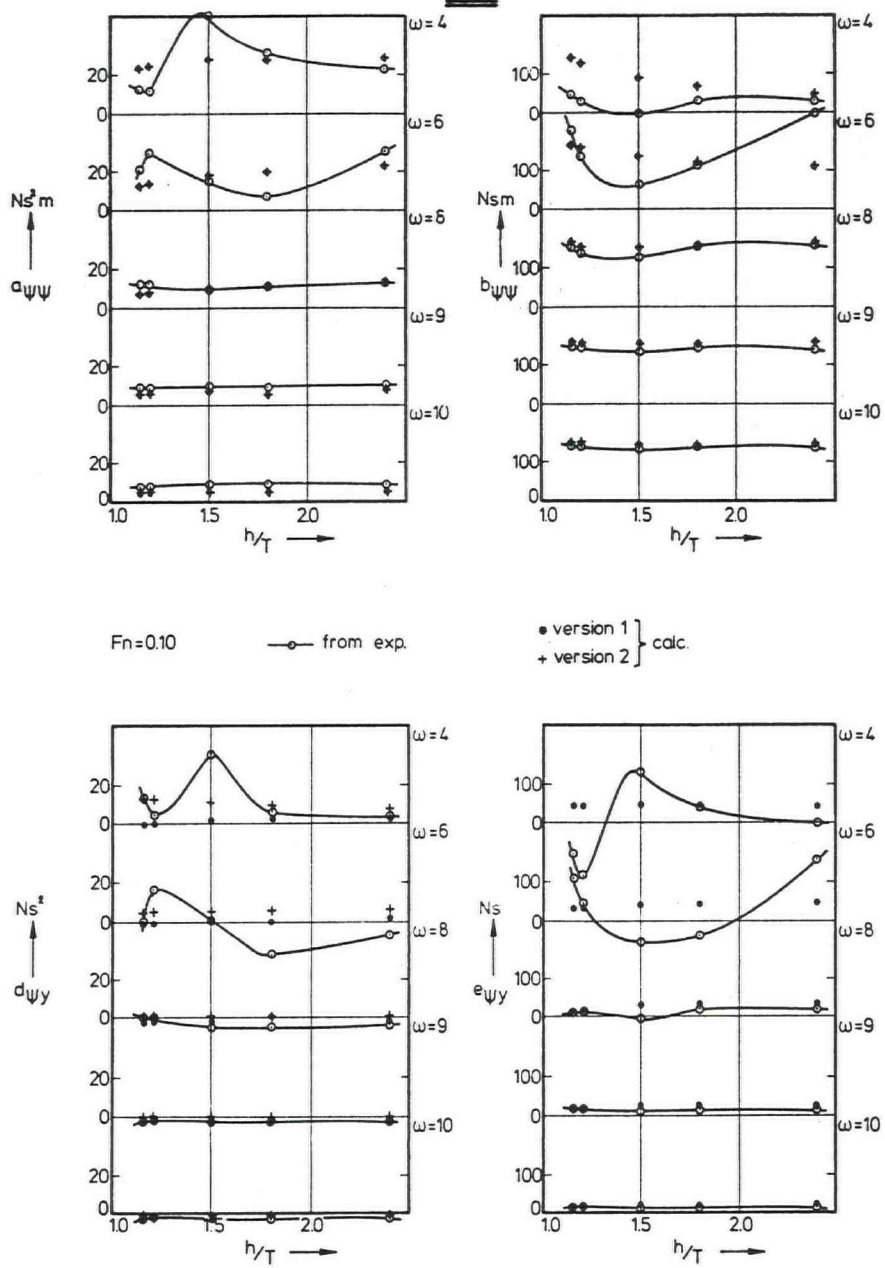


Fig.25: Comparison of experimental and calculated coefficients for yaw as a function of waterdepth-draught ratio. $F_n = 0.10$.

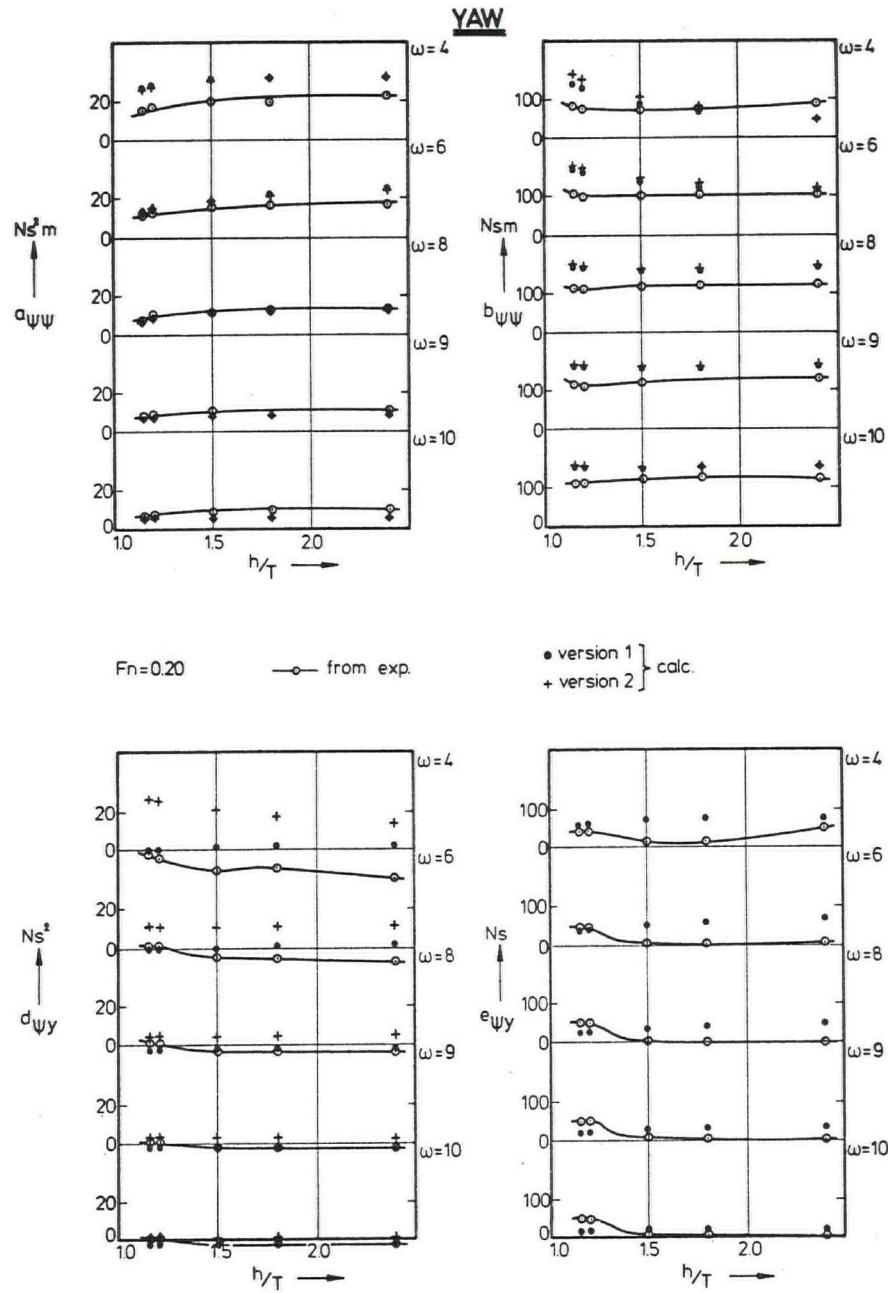


Fig.26: Comparison of experimental and calculated coefficients for yaw as a function of waterdepth-draught ratio. $Fn=0.20$.

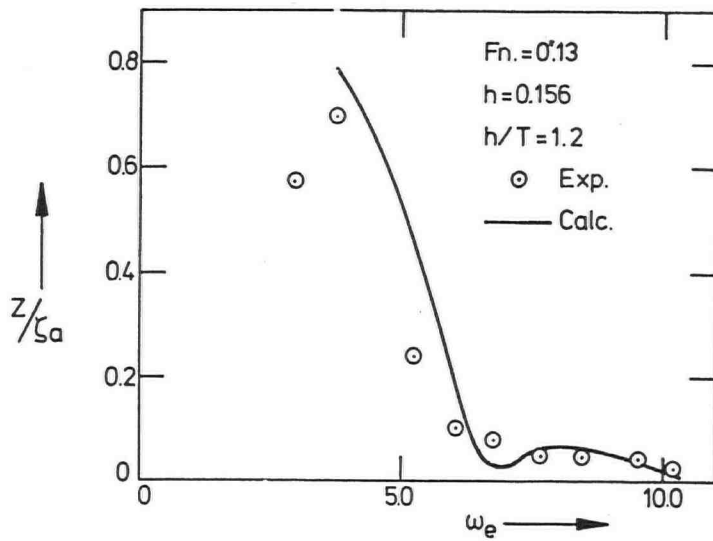


Fig. 27a: Heave amplitude response.

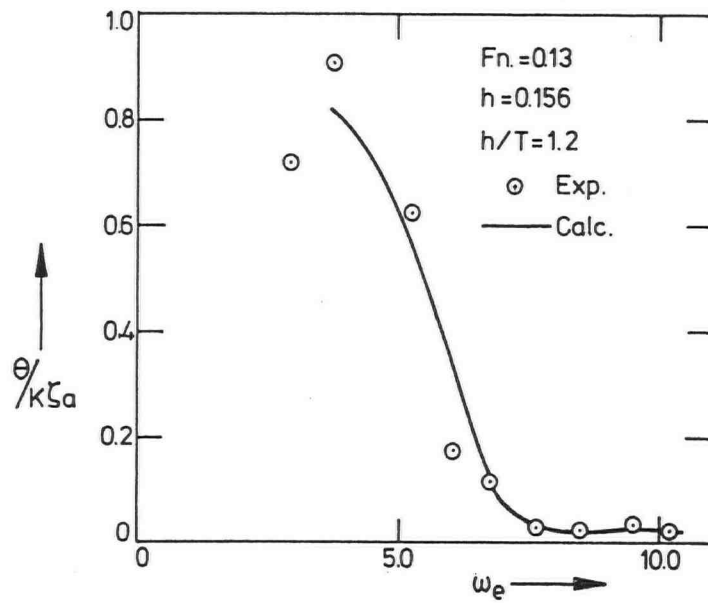


Fig. 27b: Pitch amplitude response.